IEEE Access
Multidisciplinary | Rapid Review | Open Access Journal

Received July 11, 2017, accepted August 2, 2017, date of publication August 9, 2017, date of current version May 9, 2018.

*Digital Object Identifier 10.1109/ACCESS.2017.2736978*

# Joint-Alphabet Space Time Shift Keying in mm-Wave Non-Orthogonal Multiple Access

**PANAGIOTIS BOTSINIS, (Member, IEEE), IBRAHIM HEMADEH, DIMITRIOS ALANIS, (Student Member, IEEE), ZUNAIRA BABAR, HUNG VIET NGUYEN, (Member, IEEE), DARYUS CHANDRA, (Student Member, IEEE), SOON XIN NG, (Senior Member, IEEE), MOHAMMED EL-HAJJAR, (Senior Member, IEEE), AND LAJOS HANZO, (Fellow, IEEE)**

School of Electronics and Computer Science, University of Southampton, Southampton SO17 1BJ, U.K.

Corresponding author: Lajos Hanzo (lh@ecs.soton.ac.uk)

This work was supported in part by the European Research Council under the Advanced Fellow Grant, in part by the Royal Society's Wolfson Research Merit Award, and in part by the Engineering and Physical Sciences Research Council under Grant EP/L018659/1. All data supporting this study are openly available from the University of Southampton repository at https://doi.org/10.5258/SOTON/xxxxx, https://doi.org/10.5258/SOTON/D0241, and https://doi.org/10.5258/SOTON/D0242.

**ABSTRACT** Flexible modulation schemes and smart multiple-input multiple-output techniques, as well as low-complexity detectors and preprocessors may become essential for efficiently balancing the bit error ratio performance, throughput, and complexity tradeoff for various application scenarios. Millimeter-Wave systems have a high available bandwidth and the potential to accommodate numerous antennas in a small area, which makes them an attractive candidate for future networks employing spatial modulation and space-time shift keying (STSK). Non-Orthogonal Multiple Access (NOMA) systems are capable of achieving an increased throughput, by allowing multiple users to share the same resources at the cost of a higher transmission power, or an increased detection (preprocessing) complexity at the receiver (transmitter) of an uplink (downlink) scenario. In this paper, we propose the new concept of joint-alphabet space time shift keying. As an application scenario, we employ it in the context of the uplink of NOMA mm-Wave systems. We demonstrate with the aid of extrinsic information transfer charts that a higher capacity is achievable when compared with STSK, while retaining the attractive flexibility of STSK in terms of its diversity gain and coding rate. Finally, we conceive quantum-assisted detectors for reducing the detection complexity, while attaining a near-optimal performance, when compared with the optimal iterative maximum *A posteriori* probability detector.

**INDEX TERMS** Computational complexity, Dürr-Høyer algorithm, EXIT charts, Grover's quantum search algorithm, interleave division multiple access, mm-wave, multiuser detection, quantum computing, space time shift keying.

## I. LIST OF ABBREVIATIONS

| | |
|---|---|
| AA | Antenna Array |
| AAC | Antenna Array Combination |
| ABF | Analog BeamForming |
| ACS | Add-Compare-Select |
| AE | Antenna Element |
| ASU | Antenna Selection Unit |
| AWGN | Additive White Gaussian Noise |
| AWGN | Additive White Gaussian Noise |
| BER | Bit Error Ratio |
| BLER | BLock Error Ratio |
| BS | Base Station |
| CDMA | Code Division Multiple Access |
| CF | Cost Function |
| CFE | Cost Function Evaluation |
| CIR | Channel Impulse Response |
| DCMC | Discrete-input Continuous-output Memoryless Channel |
| DHA | Dürr-Høyer Algorithm |
| DS | Direct Sequence |
| EXIT | EXtrinsic Information Transfer |
| FBKT | Forward and Backward Knowledge Transfer |
| FD-CHTF | Frequency Domain CHannel Transfer Function |
| GSTSK | Generalized Space Time Shift Keying |
| HIHO | Hard-Input Hard-Output |
| IDMA | Interleave Division Multiple Access |

| | |
|---|---|
| IFFT | Inverse Fast Fourier Transform |
| IoT | Internet of Things |
| IrCC | Irregular Convolutional Code |
| JA | Joint Alphabet |
| JA-STSK | Joint Alphabet based Space Time Shift Keying |
| LLR | Log Likelihood Ratio |
| MAP | Maximum A Posteriori probability |
| MC | Multi-Carrier |
| MFAA | Multi-Functional Antenna Array |
| MI | Mutual Information |
| ML | Maximum Likelihood |
| MS-STSK | Multi-Set Space Time Shift Keying |
| MUA | MUlti-input Approximation |
| NOMA | Non-Orthogonal Multiple Access |
| OFDM | Orthogonal Frequency Division Multiplexing |
| OFDMA | Orthogonal Frequency Division Multiple Access |
| PSK | Phase Shift Keying |
| QAM | Quadrature Amplitude Modulation |
| QMUD | Quantum-asssisted Multi-User Detector |
| QoS | Quality of Service |
| RF | Radio Frequency |
| RSC | Recursive Systematic Convolutional |
| SISO | Soft-Input Soft-Output |
| SM | Spatial Modulation |
| STSK | Space Time Shift Keying |
| URC | Unity Rate Code |

## II. INTRODUCTION

### A. MOTIVATION

The evident proliferation of wireless devices and the amount of data that is exchanged is expected to be further increased with the wide-spread introduction of the Internet of Things (IoT) and the availability of 4K resolution videos on laptops, tablets and mobile phones. Advanced MIMO and modulation techniques [1], [2], such as Spatial Modulation (SM) [3], Space Time Shift Keying (STSK) [4]–[6], or Multi-Set STSK (MS-STSK) [7], [8] will be even more essential in the future wireless systems, where a substantially increased throughput will be required, compared to the current wireless generation.

The advanced MIMO techniques will be essential in mm-Wave systems [9]–[13], for mitigating their high path loss and shadowing losses due to their high carrier frequencies [11]. At the same time, the mm-Wave systems favor the employment of such advanced MIMO and modulation techniques, which allow us to use Multi-Functional Antenna Arrays (MFAA) [14] in a compact space. Different subgroups of antennas forming the MFAA may be used for spatial multiplexing, transmit diversity or beamforming, for supporting flexibility in the design of the transceiver at mm-Wave frequencies. Therefore, the availability of MFAAs at both the transmitter and the receiver facilitates the employment of STSK, MS-STSK, as well as of the proposed Joint Alphabet STSK (JA-STSK) and Joint Alphabet MS-STSK (JA-MS-STSK). As it will be detailed in Section III, the JA-aided MIMO schemes subsume the existing STSK techniques, equipping them with an extra design parameter, which is the varying number of antennas that may be activated at any channel use. This may facilitate the reduction of the required number of Radio Frequency (RF) chains at the transmitter, which would impose a high cost reduction in the design of a wireless communication transceiver.

### B. APPLICATION SCENARIO

The currently used multiple access schemes orthogonally separate the users supported. For example, the Code Division Multiple Access (CDMA) scheme in the third generation (3G) networks separates the users by allocating a unique orthogonal spreading code to each of them, while the Orthogonal Frequency Division Multiple Access (OFDMA) scheme in the fourth generation (4G) networks achieves orthogonality between the users by allowing only a single user to transmit on a specific subcarrier. By employing Non-Orthogonal Multiple Access (NOMA) systems [15]–[19] we may be able to increase the systems' achievable throughput, since more users will be supported by the system, albeit at the cost of increasing the Base Station's (BS) detection complexity. A mm-Wave system may rely on a NOMA scheme in order to support more users at the same time in dense networks, as discussed in [20] in the context of random beamforming aided mm-Wave NOMA systems.

By allowing $U$ number of users to share the same time, frequency, space or code resources in the uplink of a NOMA system, the system's throughput may be increased by a factor of $U$, compared to the existing orthogonal multiple access systems. However, this is achieved at the cost of introducing multi-user interference, which requires the employment of powerful but complex multi-user detectors for attaining the required Quality of Service (QoS). Smart multiple access techniques may be introduced for minimizing the correlation amongst the different users' signals, which reduces the multi-user interference. In our contribution, as an application scenario we opt for Multi-Carrier Interleave Division Multiple Access (MC-IDMA) systems [21]–[26], where the users communicate with the BS over the same subcarriers during the same time slots, while each user is allocated a unique, user-specific interleaving sequence. MC-IDMA is quite similar to the state-of-the-art OFDMA, only distinguished by its different subcarrier allocation methodology and by invoking unique, user-specific interleaving sequences. It should be noted that the proposed JA-aided MIMO scheme is also applicable to other multiple access systems.

### C. SPATIAL MODULATION

In SM [3], [27], [28], the information symbols are conveyed both by the classic modulation constellations as well as by a second subchannel, where for example one out of $M$ antennas is activated for implicitly conveying $\log_2(M)$ bits. Then the receiver has to determine both the specific activated transmit antenna as well as the transmitted classic symbol.

The SM philosophy has two substantial benefits, namely the reduced number of RF chains, which reduces both the cost and the complexity of the MIMO system, and the reduced single-stream detection complexity [29], [30]. However, it is widely agreed that in its original form, SM does not achieve any transmit diversity gain, hence this has to be achieved at the receiver side. Nevertheless, it was demonstrated in [3], [31], and [32] that the SM scheme is capable of outperforming many other MIMO arrangements. The SM structure was combined with Orthogonal Frequency Division Multiplexing (OFDM) in [33], where the authors activated all antennas over all sub-carriers to transmit both the classic Phase Shift Keying (PSK) / Quadrature Amplitude Modulation (QAM) symbol over the selected Antenna Element (AE), as well as zeros representing the inactive AEs. Inspired by the philosophy of SM, Abu-Alhiga and Haas proposed the sub-carrier Index Modulation (IM) scheme [34], where the OFDM sub-carriers are activated and deactivated relying on on-off keying for implicitly conveying extra information. In [35] it was shown that if a single RF chains is desired at the transmitter, then only single carrier systems may be combined with SM, since multi-carrier systems require each transmit antenna to be connected to its own RF chain.

In [36], a Joint Alphabet (JA) design was proposed for the SM scheme, where the classic constellation and the antenna constellations were designed jointly. By choosing multiple antennas from the full set of legitimate antenna combinations, the number of legitimate combinations is increased compared to conventional SM and hence the throughput of the system is improved. This JA-SM scheme was shown to outperform the SM scheme [36] in terms of the achievable Bit Error Ratio (BER) performance.

### D. SPACE-TIME SHIFT KEYING

The STSK scheme [4]–[6] constitutes a different version of SM, which transmits a codeword over $M$ transmit antennas and $T$ time slots. More specifically, the STSK codeword is constructed by a PSK / QAM symbol spread across both the spatial and temporal domains by a linear dispersion matrix [37]. The bit stream is transformed into two parallel streams, where one selects the specific PSK / QAM symbol from a classic symbol constellation and the other bit stream determines the specific dispersion matrix from the legitimate set of matrices. Therefore, the STSK scheme may be considered as a combination of linear dispersion coding [37] and SM [38]. The STSK scheme exhibits numerous benefits, such as having a tunable transmit diversity gain, which is determined both by the specific number of transmit antennas and by the number of time slots used by the dispersion matrix [42]. Its throughput is also tunable, which is based on the number of dispersion matrices and on the symbol constellation size employed. The Generalised STSK (GSTSK) scheme of [40] additionally introduces a multiplexing gain, which is achieved by allowing multiple parallel streams of STSK codewords to be transmitted simultaneously by each transmitter. In order to overcome the frequency selective fading imposed by the time dispersion associated with the multipath components' delay in wideband channels, the STSK scheme was amalgamated with OFDM [39], [41].

### E. MULTI-SET SPACE-TIME SHIFT KEYING

The MS-STSK scheme of [7] and [8] combines STSK and SM by introducing an additional degree of freedom into the system's throughput. More specifically, the MS-STSK scheme employs $M$ transmit RF chains and $N_T > M$ transmit Antenna Arrays (AA), essentially allowing a third parallel bit stream to determine the specific antenna combination, which will transmit the STSK codeword. However, in multi-carrier systems every transmit AA has to be connected to an RF chain ($N_T = M$), due to the employment of the Inverse Fast Fourier Transform (IFFT), which maps the frequency domain symbols to the time domain [35]. The main contributions to the development of the STSK scheme are gathered in Table 1.

The concept of multiple AAs and the multiple antenna elements of each AA may be physically implemented as a single MFAA, as discussed in [14]. More specifically, in an MFAA different groups of antenna elements may form different virtual AAs, which may be used for MIMO schemes. At the same time, the multiple antenna elements of each AA may also be exploited for beamforming. Therefore, the MFAAs may be designed for achieving the required trade-offs between spatial multiplexing, spatial diversity and beamforming.

### F. NOVEL CONTRIBUTIONS

*Against this background, our novel contributions are:*

1) *We propose the Joint Alphabet based Space Time Shift Keying (JA-STSK), where a variable fraction of the maximum number of RF chains may be active in order to transmit an STSK codeword. In contrast to the JA-SM of [36], which employs different antenna combinations along with the same scalar symbols transmitted by each antenna, the JA-STSK scheme creates the joint alphabet by using different dispersion matrices and antenna combinations over multiple time slots, essentially maintaining the advantages of STSK over SM. More specifically, an alphabet consists of a specific number of active RF chains, the legitimate AA Combinations (AAC), a symbol constellation and a set of dispersion matrices. The joint alphabet is created by the superset of the different alphabets.*
2) *We demonstrate that JA-STSK results in a higher achievable capacity than STSK in the context of both our multi-carrier and single-carrier NOMA applications scenarios, as well as exhibiting a higher design flexibility. In our contribution, the multi-carrier and single-carrier NOMA systems are represented by the MC-IDMA and SC-IDMA systems, respectively, where multiple users transmit during the same time slot over all available subcarriers. We also propose the JA-MS-STSK scheme, which may be employed in single carrier*

**TABLE 1. Major contributions conceived for the STSK scheme.**

| Authors | Year | Contribution |
|---|---|---|
| Hassibi and Hochwald [37] | 2001 | Proposed the linear dispersion code scheme, which is capable of striking a design trade-off between the attainable diversity gain and achievable throughput. |
| Sugiura *et al.* [38] | 2011 | Introduced the STSK concept by combining both SM and LDC. |
| Driusso *et al.* [39] | 2012 | Combined STSK with OFDM in order to transmit over the wideband channel. |
| Sugiura *et al.* [40] | 2012 | Introduced the GSTSK scheme, where multiple dispersion matrices are simultaneously activated by different symbols. |
| Kadir *et al.* [41] | 2013 | Proposed a new bit-to-symbol mapping technique for OFDM-STSK. Combined STSK with both OFDMA and SC-FDMA for operating in multi-user scenarios over frequency-selective channels. |
| Hemadeh *et al.* [13] | 2016 | Amalgamated STSK and SM associated with codeword preprocessing and with a reduced complexity detector. |
| Hemadeh *et al.* [7] | 2016 | Proposed the MS-STSK scheme, along with a hard-output reduced-complexity detector. |
| Hemadeh *et al.* [8] | 2017 | Introduced an iterative soft-input soft-output detector for MS-STSK in the context of multi-carrier mm-Wave systems. |

*systems, again, exhibiting a higher capacity than STSK. It should be noted that since both the JA-STSK and JA-MS-STSK are MIMO schemes, they are applicable in both single user and multi-user systems. Furthermore, even though mm-Wave carrier frequencies are suitable for JA-STSK, due to the ability of accommodating multiple antennas in a compact space, the proposed schemes may also be employed at any carrier frequencies. We opted for demonstrating the proposed concepts in NOMA mm-Wave systems, inspired by our vision that these systems may become the most popular multiple access schemes in future wireless generations.*

3) *We present a novel methodology for selecting the AACs in JA-STSK, MS-STSK and JA-MS-STSK, which increases the achievable capacity, when compared to a random selection of AACs. Since not all antenna combinations of these schemes are legitimate in each alphabet, the specific methodology followed for selecting the legitimate subset of antenna combinations affects the system's performance.*
4) *We demonstrate that the Hard-Input Hard-Output (HIHO) and Soft-Input Soft-Output (SISO) Quantum-assisted Multi-User Detectors (QMUD) of [26], [43]–[45] may also be used in mm-Wave MC-IDMA systems, where the number of transmit AAs is higher than the number of receive AAs and the JA-STSK is used. The resultant systems exhibit a near-optimal performance, approaching that of the optimal Maximum A Posteriori probability (MAP) MUD. We show for the first time that an EXtrinsic Information Transfer (EXIT) chart-aided irregular design [46] is possible for the SISO QMUD with the aid of Irregular Convolutional Codes (IrCC), in order to operate close to the achievable capacity.*

The paper is structured as follows. In Section IV, we analyse the mm-Wave MC-IDMA system model, including the proposed JA-STSK encoding process at the users' terminals, as well as the MUD and iterative decoding process at the BS. In Section V, we quantify the achievable capacity and the attainable gains, while in Section VI we conceive a novel antenna selection methodology for the joint alphabet. The simulation results of the JA-STSK assisted mm-Wave MC-IDMA systems relying on our QMUD and IrCC are discussed in Section VII. Finally, our conclusions are offered in Section VIII.

## III. JOINT ALPHABET SPACE-TIME SHIFT KEYING

Let us commence by investigating a single-user single-carrier system employing STSK, MS-STSK, JA-STSK and JA-MS-STSK before analyzing the joint alphabet schemes in a multi-user mm-Wave system. Let us also consider an example scenario to accompany the general description of the system. All parameters of the scenario are stated in Table 2, where we may observe that the specific parameter values of the scenario may change depending on which system is investigated. In all systems, $T = 2$ time slots and $N_t = 5$ transmit antennas

**TABLE 2. Parameters of the STSK schemes in the single-user single-carrier scenario.**

| | STSK | MS-STSK | JA-STSK | JA-MS-STSK |
|---|---|---|---|---|
| Number of RF chains | $M = 5$ | | | |
| Number of time slots | $T = 2$ | | | |
| Number of transmit antennas | $N_t = 5$ | $N_t = 10$ | $N_t = 5$ | $N_t = 10$ |
| Number of dispersion matrices | $Q = 8$ | | – | |
| Symbol constellation size | $L = 4$ | | – | |
| Number of levels | – | | $V = 5$ | |
| Number of dispersion matrices on the $v$th level | – | | $Q_v = \{0, 2, 4, 8\}$ | |
| Symbol constellation size on the $v$th level | – | | $L_v = \{0, 2, 4, 8\}$ | |
| Number of antennas activated on the $v$th level ($\leq M$) | – | | $D_v = \{1, 2, 3, 4, 5\}$ | |
| Number of antenna combinations | – | $K = 2^{\left\lfloor \log_2 \left[ \binom{5}{3} \right] \right\rfloor} = 128$ | – | |
| Number of antenna combinations on the $v$th level, each activating $D_v$ antennas | – | | $K_v = \{0, 1, 2, 3, 4\}$ | |

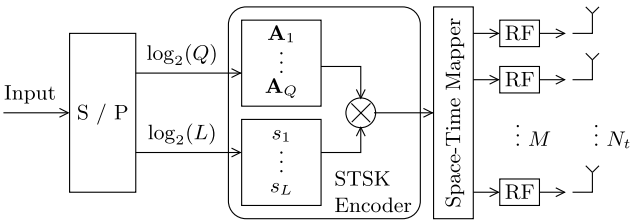


**FIGURE 1. Block diagram of the STSK scheme at the transmitter of a single-carrier system, where two parallel bit streams determine the specific dispersion matrix $\mathbf{A}_q$ and classic constellation symbol $s_l$, which eventually create the STSK codeword. The STSK codeword is transmitted by all $M$ available RF chains via all $N_t = M$ available antennas.**

are used for transmitting a (JA-MS-)STSK codeword. In the STSK and JA-STSK scenarios, $M = N_t = 5$ RF chains are available, while only $M = 3$ RF chains are used in MS-STSK and JA-MS-STSK. Please note that the rest of the parameters in Table 2 will be gradually introduced in our analysis. Furthermore, in the context of single-carrier systems we will refer to antennas, while in multi-carrier mm-Wave systems we will refer to AAs, where each AA may have multiple AEs for performing analog beamforming.

### A. STSK IN SINGLE-USER SINGLE-CARRIER SYSTEMS

#### 1) TRANSMITTER

In a single-user single-carrier scenario, the STSK scheme spreads a selected information symbol over space, in terms of the available transmit antennas, as well as time, in terms of time slots, by using a dispersion matrix selected from a pool of appropriately designed dispersion matrices, as shown in Fig. 1. In STSK it is obligatory to form two parallel bit streams, where the first parallel bit stream selects a $(M \times T)$-element dispersion matrix $\mathbf{A}_q$ with $q = 1, \ldots, Q$, based on a set of $\log_2(Q)$ bits, while the second one selects the classic $L$-ary PSK / QAM information symbol $s_l$ with $l = 1, \ldots, L$, based on a set of $\log_2(L)$ bits, as exemplified in Fig. 1. The resultant $(M \times T)$-element STSK codeword $\mathbf{X}_{q,l}$, which is constructed by the $q$th dispersion matrix $\mathbf{A}_q$ and the $l$th information symbol $s_l$ is

$$\mathbf{X}_{q,l} = \mathbf{A}_q \cdot s_l. \tag{1}$$

Since there are $Q$ dispersion matrices and $L$ scalar information symbols, there may be $(Q \times L)$ legitimate STSK codewords. In the STSK scenario of Table 2, where $M = N_t = 5$ and $T = 2$, the $(N_t \times T) = (5 \times 2)$-element STSK codeword of the $q$th dispersion matrix and the $l$th information symbol is

$$\mathbf{X}_{q,l} = \begin{bmatrix} a_q^{(11)} & a_q^{(12)} \\ a_q^{(21)} & a_q^{(22)} \\ a_q^{(31)} & a_q^{(32)} \\ a_q^{(41)} & a_q^{(42)} \\ a_q^{(51)} & a_q^{(52)} \end{bmatrix} \cdot s_l, \tag{2}$$

where $a_q^{(i,j)}$ is the element of the $q$th dispersion matrix $\mathbf{A}_q$ on the $i$th row and the $j$th column.

The dispersion matrices in this paper were designed based on the rank- and determinant-criterion of [14], but an improved performance is expected if they are designed based on the maximization of the Discrete-input Continuous-output Memoryless Channel (DCMC) capacity [14], or on the minimization of the BLock Error Ratio (BLER) [47]. The power constraint of

$$tr\left\{\mathbf{A}_q^H \mathbf{A}_q\right\} = T \tag{3}$$

is satisfied for each of the generated dispersion matrices for achieving a unity average transmission power over $T$ time slots.

#### 2) RECEIVER

When the codeword is transmitted by the $N_t = M$ transmit antennas over fading channels, the $(N_r \times T)$-element signal

$\mathbf{Y}$ received at the $N_r$ receive antennas over $T$ time slots is

$$\mathbf{Y} = \mathbf{H} \cdot \mathbf{X}_{q,l} + \mathbf{N}, \tag{4}$$

where the $(N_r \times N_t)$-element matrix includes the channel states and $\mathbf{N}$ is the $(N_r \times T)$-element Additive White Gaussian Noise (AWGN) matrix, where each element has zero mean and a variance of $N_0$. Additionally, in this contribution we assume quasi-static channels, which exhibit the same channel states over $T$ time slots, enabling the representation of (4).

#### 3) STSK CODEWORD DETECTION

The Maximum Likelihood (ML) detector may be employed at this point at the receiver in order to determine, which specific STSK codeword was transmitted, given that $\mathbf{Y}$ of (4) contains the signals received over $T$ time slots. The estimated codeword $\bar{X}$ is found according to

$$\bar{\mathbf{X}} = \arg\min_{\mathbf{X}} \|\mathbf{Y} - \mathbf{H} \cdot \mathbf{X}\|^2, \tag{5}$$

which is equivalent to

$$\{\bar{q}, \bar{l}\} = \arg\min_{q,\, l} \left\|\mathbf{Y} - \mathbf{H} \cdot \mathbf{A}_q \cdot s_l\right\|^2. \tag{6}$$

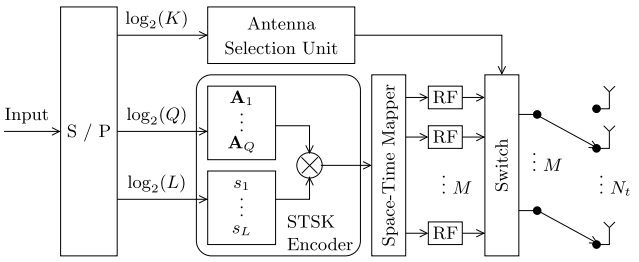


**FIGURE 2. Block diagram of the MS-STSK scheme at the transmitter of a single-carrier system, where the first parallel bit stream determines the antenna combination that will be activated in order to transmit the STSK codeword. The second and third parallel bit streams determine the specific dispersion matrix $\mathbf{A}_q$ and classic constellation symbol $s_l$, which eventually create the STSK codeword. Only $M$ out of $N_t$ antennas are activated for the transmission of each STSK codeword.**

### B. MULTI-SET STSK IN SINGLE-USER SINGLE-CARRIER SYSTEMS

#### 1) TRANSMITTER

In a single-carrier system, MS-STSK [7] may be used when there are fewer RF chains than transmit antennas ($M < N_t$). As shown in Fig. 2, in the MS-STSK scheme [7], there are three parallel bit streams that determine the transmitted signal. More specifically, the last $B_{STSK} = \log_2(L) + \log_2(Q) = \log_2(L \cdot Q)$ bits select the STSK codeword by spreading an $L$-ary PSK / QAM symbol over $T$ time slots using one of the $Q$ available dispersion matrices, in exactly the same way as in Section III-A. At the same time, the first $B_{ASU} = \log_2(K)$ bits enter the Antenna Selection Unit (ASU) and choose the antennas from which the selected STSK codeword will be transmitted. Since there are $M$ RF chains, the STSK codeword will be transmitted by $M$ out of the $N_t$ available antennas and the number of antenna combinations is $\binom{N_t}{M}$. Since the number of antenna combinations $K$ should be a power of 2, in order to have a one-to-one mapping of $\log_2(K)$ to a unique antenna combination, the maximum number of legitimate antenna combinations, when there are $N_t$ transmit antennas and $M$ RF chains is

$$K = 2^{\left\lfloor \log_2\left[\binom{N_t}{M}\right]\right\rfloor} = 2^{B_{ASU}}. \tag{7}$$

In our MS-STSK scenario of Table 2, where $N_t = 5$ and $M = 3$, there are $K = 8$ legitimate antenna combinations and $B_{ASU} = \lfloor \log_2(K) \rfloor = 3$ bits will determine the specific antenna combination.

When the $q$th dispersion matrix $\mathbf{A}_l$ is selected to spread the $l$th information symbol $s_l$ over $M$ RF chains and $T$ time slots, while the resultant STSK codeword is transmitted by the $k$th antenna combination, the $(N_t \times T)$-element output of the transmitter $\mathbf{X}_{k,q,l}$ is

$$\mathbf{X}_{k,q,l} = \mathbf{Z}_k \cdot \mathbf{A}_q \cdot s_l, \tag{8}$$

where the $(N_t \times M)$-element matrix $\mathbf{Z}_k$ encapsulates the choice of the antenna combination. More specifically, the $(n_t, m)$th element of the matrix $\mathbf{Z}_k$ is equal to 1 if the $m$th spatial dimension of the STSK codeword will be transmitted by the $n_t$th transmit antenna, otherwise it is equal to 0 as stated in

$$z_k^{(n_t,m)} = \begin{cases} 1, & n_t\text{th antenna transmits the } m\text{th row} \\ 0, & \text{otherwise.} \end{cases} \tag{9}$$

This is a mapping that is determined by the ASU of Fig. 2, hence there are $K$ legitimate $\mathbf{Z}_k$ matrices.

In our MS-STSK scenario of Table 2, where $M = 5$, $N_t = 10$, $T = 2$ and $K = 128$, let us assume that the $k = 2$nd antenna combination is $\kappa_k = \kappa_2 = [2, 4, 5, 8, 10]$, where the order the antenna indices appear in the antenna combinations $\kappa_k$ determines the STSK codeword's spatial dimension that will be mapped to them. In this example the $m = 1$st row of the STSK codeword will be mapped to antenna #2, while the $m = 2$nd, 3rd, 4th and 5th rows of the STSK codeword will be mapped to antennas #4, #5, #8 and #10, respectively. The resultant antenna combination matrix $\mathbf{Z}_2$ is:

$$\mathbf{Z}_2 = \begin{bmatrix} 0 & 0 & 0 & 0 & 0 \\ 1 & 0 & 0 & 0 & 0 \\ 0 & 0 & 0 & 0 & 0 \\ 0 & 1 & 0 & 0 & 0 \\ 0 & 0 & 1 & 0 & 0 \\ 0 & 0 & 0 & 0 & 0 \\ 0 & 0 & 0 & 0 & 0 \\ 0 & 0 & 0 & 1 & 0 \\ 0 & 0 & 0 & 0 & 0 \\ 0 & 0 & 0 & 0 & 1 \end{bmatrix}. \tag{10}$$

Hence, assuming that the $q$th dispersion matrix $\mathbf{A}_q$, spreads the $l$th information symbol $s_l$, and that the $k = 2$nd antenna combination is selected, represented by $\mathbf{Z}_2$ in (10), the output

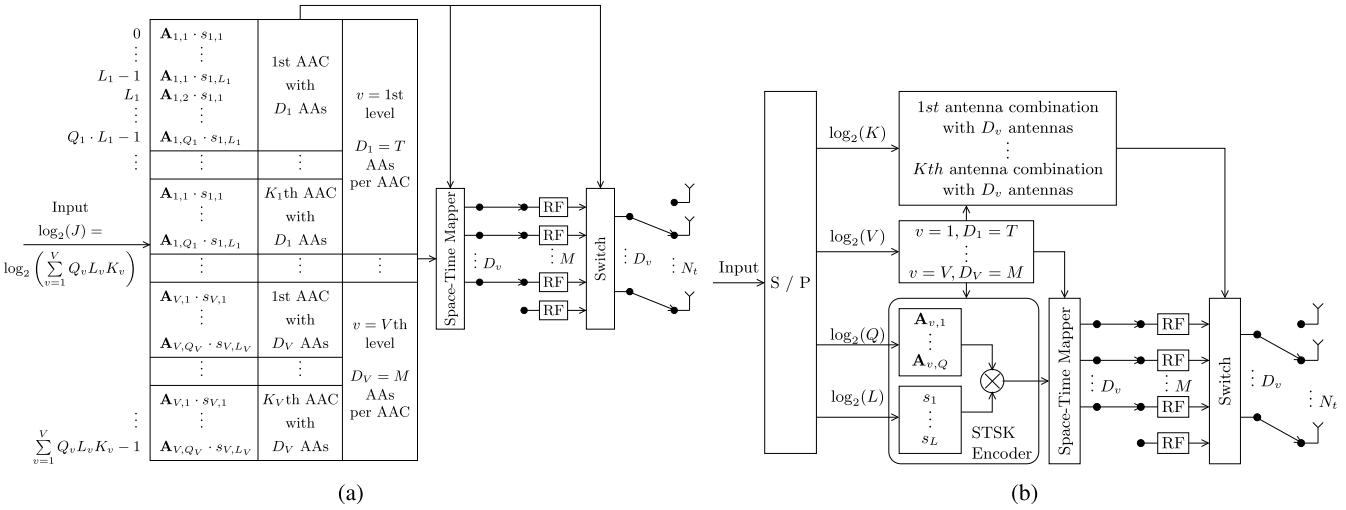


**FIGURE 3.** Two block diagrams of the JA-STSK scheme, where in (a) a single stream determines the JA-STSK codeword, removing the requirement of having the same number of dispersion matrices $Q_V$, symbol constellation size $L_V$ and number of antenna combinations $K_V$ on each level $v$. On the other hand, this requirement is still valid in (b), where four parallel bit streams construct the JA-STSK codeword, which uses $Q$ dispersion matrices, a constellation size of $L$ symbols and $K$ antenna combinations on each level $v$. The number $D_V$ of AAs activated on the $v$th level is the same in both architectures. We have also assumed $T < M$, in order for the lowest level to activate $T$ RF chains and for the highest level to activate $M$ RF chains.

of the transmitter $\mathbf{X}_{k,q,l} = \mathbf{X}_{2,q,l}$ in our scenario is

$$\mathbf{X}_{2,q,l} = \mathbf{Z}_2 \cdot \mathbf{A}_q \cdot s_l = \begin{bmatrix} 0 & 0 \\ a_q^{(11)} & a_q^{(12)} \\ 0 & 0 \\ a_q^{(21)} & a_q^{(22)} \\ a_q^{(31)} & a_q^{(32)} \\ 0 & 0 \\ 0 & 0 \\ a_q^{(41)} & a_q^{(42)} \\ 0 & 0 \\ a_q^{(51)} & a_q^{(52)} \end{bmatrix} \cdot s_l, \qquad (11)$$

where again $a_q^{(i,j)}$ is the element of the $q$th dispersion matrix $\mathbf{A}_q$ on the $i$th row and the $j$th column. It should be noted that the selection of $K$ legitimate antenna combinations out of $\binom{N_t}{M} > K$ antenna combinations affects the system's performance, since there exists a correlation between the use of the same antenna in different antenna combinations.

### 2) RECEIVER

The received signal at the $N_r$ receive antennas is represented by the $(N_r \times T)$-element complex matrix $\mathbf{Y}$, which is described as

$$\mathbf{Y} = \mathbf{H} \cdot \mathbf{X}_{k,q,l} + \mathbf{N}, \qquad (12)$$

where, similarly to (4), the $(N_r \times N_t)$-element matrix $\mathbf{H}$ includes the quasi-static channel gains and $\mathbf{N}$ represents the AWGN with zero mean and a variance of $N_0$. Comparing (4) and (12), the main difference is that only a subset of the transmit antennas are actually transmitting a signal in the latter case.

### 3) MS-STSK CODEWORD DETECTION

Since the receiver is aware of the legitimate antenna combinations that the transmitter has used, it may proceed to perform a hard ML detection of the transmitted MS-STSK codeword, in a similar way as in the STSK case of (5). More specifically, the estimated MS-STSK codeword may be found based on

$$\{\bar{k}, \bar{q}, \bar{l}\} = \arg\min_{k,q,l} \left\| \mathbf{Y} - \mathbf{H} \cdot \mathbf{Z}_k \cdot \mathbf{A}_q \cdot s_l \right\|^2. \qquad (13)$$

## C. JOINT ALPHABET STSK

The proposed JA-STSK and JA-MS-STSK schemes build on the STSK and MS-STSK schemes, respectively. More specifically, the joint-alphabet based schemes may allow only a subset of the available $M$ RF chains to be activated in order to transmit an STSK codeword. In the context of both JA-STSK and JA-MS-STSK, this means that there are multiple alphabets of dispersion matrices, which may spread the scalar information symbol over a different number of spatial dimensions. Furthermore, it also means that not only a different antenna combination will be used during the transmission of each codeword, but also a different *number* of antennas may be activated for the transmission.

It should be noted that both the JA-STSK and JA-MS-STSK schemes are capable of creating a single joint alphabet of STSK codewords, which are not necessarily constructed by independent parallel bit streams in contrast to STSK of Fig. 1, as presented in Fig. 3a. Similarly, the proposed JA-MS-STSK scheme may also create a single joint alphabet in the same way as the JA-STSK scheme. It should be noted that if needed, the joint alphabets in both the JA-STSK and the JA-MS-STSK can be assigned to parallel bit streams, making the JA-aided STSK a superset of the STSK family. More specifically, for $V = 1$, $D_V = M$ and $K = 1$, JA-STSK is equivalent to STSK, as illustrated in Fig. 3b.

**TABLE 3. Specifications of JA-STSK schemes.**

| Scheme | Parallel Input Streams | Single-Carrier Systems | Multi-Carrier Systems | Design Trade-offs |
|---|---|---|---|---|
| STSK | 2 | ✓ | ✓ | + Higher diversity than SM |
| MS-STSK | 3 | ✓ | | + Better performance than STSK<br>+ Same diversity order as STSK<br>– Requires more AAs than STSK |
| JA-STSK | $1-4$ | ✓ | ✓ | + Better performance than STSK<br>+ Same diversity order as STSK |
| JA-MS-STSK | $1-4$ | ✓ | | + Better performance than STSK, MS-STSK and JA-STSK<br>+ Same diversity order as STSK<br>– Requires more AAs than STSK |

**TABLE 4. Parameters of the JA-STSK scheme.**

| | |
|---|---|
| Number of RF chains | $M$ |
| Number of time slots | $T$ |
| Number of transmit antenna arrays | $N_t$ |
| Number of antenna elements on each transmit antenna array | $N_{AA}^t$ |
| Number of levels | $V$ |
| Number of dispersion matrices on the $v$th level | $Q_v$ |
| Symbol constellation size on the $v$th level | $L_v$ |
| Symbol constellation on the $v$th level | $\mathcal{L}_v$ |
| Number of antenna arrays activated on the $v$th level ($\leq M$) | $D_v$ |
| Number of antenna array combinations on the $v$th level, each activating $D_v$ antenna arrays | $K_v$ |
| $q$th $(D_v \times T)$-element dispersion matrix on the $v$th level | $\mathbf{A}_{v,q}$ |
| $l$th information symbol on the $v$th level | $s_{v,l}$ |
| Number of JA-STSK codewords on the $v$th level | $J_v$ |

This leads us to the concept of $V$ *alphabet levels* and the creation of a single bit stream in both JA-STSK and JA-MS-STSK for mapping the bits to the selected codewords of the joint alphabet constructed as in Fig. 3a. Table 3 portrays the discussed schemes with respect to their suitability in single-carrier and multi-carrier scenarios, as well as the number of parallel bit streams they may accept as inputs.

### 1) TRANSMITTER

Let us now focus our attention on the transmitter of the JA-STSK scheme, depicted in Fig. 3. Let us also define as the *vth level* an alphabet that includes the specific STSK codewords, which are constructed by $Q_v$ dispersion matrices and a classic symbol constellation size of $L_v$. The parameters used in our analysis are illustrated in Fig. 3a and gathered in Table 4. The values of the parameters used in our single-user single-carrier scenario are given in Table 2.

The resultant STSK codewords of the $v$th level are transmitted over $D_v \leq M$ activated transmit antennas with the aid of $K_v$ antenna combinations, where $v = 1, 2, \ldots, V$ and $V \leq M$ is predetermined. Two different levels[1] must activate a different number of antennas. In other words, the value of $D_v$ must be unique to the $v$th level. Let us define the $l$th scalar information symbol chosen by the $v$th level's symbol constellation $\mathcal{L}_v$ of size $L_v$ as $s_{v,l}$, where $l = 1, 2, \ldots, L_v$. That symbol, which is chosen by the constellation $\mathcal{L}$, is spread in time and space by the $q$th selected $(D_v \times T)$-element dispersion matrix $\mathbf{A}_{v,q}$, where $q = 1, 2, \ldots Q_v$, resulting in the $(D_v \times T)$-element STSK codeword

$$\mathbf{X}_{v,q,l} = \mathbf{A}_{v,q} \cdot s_{v,l}. \tag{14}$$

The dispersion matrix $\mathbf{A}_{v,q}$ spreads the information symbol $s_{v,l}$ over $T$ time slots and $D_v$ antennas, where the number of antennas $D_v$ is unique to each level. For example, in our single-user single-carrier scenario of Table 2, let us assume that for the $v = 3$rd level, $Q_v = Q_3 = 2$ dispersion matrices are used, as well as *BPSK* symbols, associated with $L_v = L_3 = 2$. Therefore, in our scenario, only the $v = 3$rd level can activate $D_3 = 3$ antennas. The STSK codeword $\mathbf{X}_{v,q,l}$ is then mapped to a JA-STSK codeword by exploiting the $k$th antenna combination of the $v$th level, where $k = 1, 2, \ldots, K_v$, resulting in the $(N_t \times T)$-element MS-STSK codeword

$$\mathbf{X}_j = \mathbf{Z}_{v,k} \cdot \mathbf{X}_{v,q,l} = \mathbf{Z}_{v,k} \cdot \mathbf{A}_{v,q} \cdot s_{v,l}, \tag{15}$$

where $j$ is used because we do not necessarily have an one-to-one mapping between the level, dispersion matrix, information symbol as well as the antenna combination indices and the index of the corresponding symbol in the joint alphabet, which would imply having parallel streams, as depicted in Fig. 3. Furthermore, the $(N_t \times D_v)$-element matrix $\mathbf{Z}_{v,k}$ is the antenna combination mapping matrix that allocates the input STSK codeword $\mathbf{X}_{v,q,l}$ to the corresponding antennas that compose the $k$th antenna combination of the $v$th level, leaving the rest of the antennas inactive. By comparing (15) to (8), we may observe that a set of MS-STSK codewords are generated for each alphabet level. The maximum number of

[1]Note that the terminology of a "level" is used solely for the ease of presentation, since eventually a single joint alphabet is used and the levels will hence have no physical meaning.

antenna combinations for the $v$th level is equal to

$$K_{v,\max} = \binom{N_t}{D_v}. \tag{16}$$

However, please note that we allow $K_v \leq K_{v,\max}$ in order to reduce the correlation represented by the antennas that are common in the different antenna combinations, which transmit the same STSK codeword, as it will be exemplified in Section VI. In our example, where $D_3 = 3$ antennas are activated, we expect a high correlation between two antenna combinations, where one utilizes the first, second and third antennas, and the other activates the first, second and fourth antennas, since the first and second antennas are common in both antenna combinations. Therefore, the number of legitimate JA-STSK codewords that may be created by the $v$th level is

$$J_v = Q_v \cdot L_v \cdot K_v. \tag{17}$$

In our scenario, according to (16), let us opt for choosing $K_v = K_3 = 2$ out of the maximum of $K_{v,\max} = K_{3,\max} = \binom{5}{3} = 10$ AAs combinations, to form the set of legitimate AACs. Let us assume for our scenario that the two AACs are $\kappa_1 = [1, 2, 3]$ and $\kappa_2 = [1, 2, 4]$, where $\kappa_1$ indicates that the first AAC activates the first, second and third transmit AAs out of the $N_t = 5$ available ones. Based on (17) and the fact that $Q_v = Q_3 = 2$ and $L_v = L_3 = 2$, the number of JA-STSK codewords in our scenario is $J_v = Q_v \cdot L_v \cdot K_v = 8$ and these are created according to (14) and (15), resulting in the following set for $v = 3$:

$$\mathcal{X}_{v=3} = \left\{ \begin{bmatrix} a_{v,1}^{(11)} & a_{v,1}^{(12)} \\ a_{v,1}^{(21)} & a_{v,1}^{(22)} \\ a_{v,1}^{(31)} & a_{v,1}^{(32)} \\ 0 & 0 \\ 0 & 0 \end{bmatrix} s_{v,1}, \begin{bmatrix} a_{v,1}^{(11)} & a_{v,1}^{(12)} \\ a_{v,1}^{(21)} & a_{v,1}^{(22)} \\ 0 & 0 \\ a_{v,1}^{(31)} & a_{v,1}^{(32)} \\ 0 & 0 \end{bmatrix} s_{v,1}, \ldots, \right.$$
$$\left. \begin{bmatrix} a_{v,2}^{(11)} & a_{v,2}^{(12)} \\ a_{v,2}^{(21)} & a_{v,2}^{(22)} \\ a_{v,2}^{(31)} & a_{v,2}^{(32)} \\ 0 & 0 \\ 0 & 0 \end{bmatrix} s_{v,2}, \begin{bmatrix} a_{v,2}^{(11)} & a_{v,2}^{(12)} \\ a_{v,2}^{(21)} & a_{v,2}^{(22)} \\ 0 & 0 \\ a_{v,2}^{(31)} & a_{v,2}^{(32)} \\ 0 & 0 \end{bmatrix} s_{v,2} \right\}. \tag{18}$$

By combining the sets of MS-STSK codewords of each level we may create the joint alphabet of the JA-STSK. Hence, the number of legitimate codewords $J$ would be equal to

$$J = \sum_{v=1}^{V} J_v = \sum_{v=1}^{V} Q_v \cdot L_v \cdot K_v. \tag{19}$$

It should be noted that the number of codewords in the joint alphabet $J$ should be equal to a power of 2, since a distinct number of bits should be mapped to a codeword. However, the value $J_v$ in (19), does not necessarily correspond to a power of 2, as discussed in Fig. 3a. Therefore, the number of bits that the JA-STSK scheme maps to a single codeword is

$$B = \log_2(J) = \log_2\left(\sum_{v=1}^{V} Q_v \cdot L_v \cdot K_v\right), \tag{20}$$

Hence, the $(N_t \times T)$-element JA-STSK codeword $\mathbf{X}$ transmitted by the $u$th user belongs to its associated joint alphabet, as encapsulated in

$$\mathbf{X} = \{\mathcal{X}_1, \ldots, \mathcal{X}_V\} \tag{21}$$

#### 2) RECEIVER

The transmitted JA-STSK codeword may be described similarly to the reception of the MS-STSK codeword of (12) as in

$$\mathbf{Y} = \mathbf{H} \cdot \mathbf{X}_j + \mathbf{N}, \tag{22}$$

where the $(N_r \times T)$-element matrix $\mathbf{Y}$ contains the received signals at the $N_r$ receive antennas over $T$ time slots, the $(N_r \times N_t)$-element matrix $\mathbf{H}$ includes the quasi-static channel states, the $(N_t \times T)$-element $\mathbf{X}_j$ is one of the $J$ number of STSK codewords given in (21) and $\mathbf{N}$ is the $(N_r \times T)$-element AWGN matrix.

#### 3) JA-STSK CODEWORD DETECTION

The transmitted JA-STSK codeword may be estimated using the ML detector as in

$$\bar{\mathbf{X}}_j = \arg\min_{\mathbf{X}_j} \left\| \mathbf{Y} - \mathbf{H} \cdot \mathbf{X}_j \right\|^2, \tag{23}$$

where the subscript $j$ uniquely corresponds to a single JA-STSK codeword of (21). The ML detector of (23) corresponds to the general case of Fig. 3a, where there are no parallel input bit streams to the JA-STSK encoder. In the special case of Fig. 3b, where parallel bit streams determine the alphabet level $v$, the antenna combination $\mathbf{Z}_{v,k}$, the dispersion matrix $\mathbf{A}_{v,q}$ and the $L_v$-ary PSK / QAM symbol $s_{v,l}$, the ML detector may be described as

$$\left\{\bar{v}, \bar{k}, \bar{q}, \bar{l}\right\} = \arg\min_{v,k,q,l} \left\| \mathbf{Y} - \mathbf{H} \cdot \mathbf{Z}_{v,k} \cdot \mathbf{A}_{v,q} \cdot s_{v,l} \right\|^2. \tag{24}$$

Please note that (24) implies that in each level $v = 1, \ldots, V$, we employ same number of antenna combinations $K_v = K$, dispersion matrices $Q_v = Q$ and the same constellation size $L_v = L$, for $v = 1, \ldots, V$, which is a special case of the proposed JA-STSK scheme. In the following application scenario, we employ the general case, where each level may employ a different number of antenna combinations, dispersion matrices and constellation.

## IV. mm-WAVE MC-IDMA APPLICATION SCENARIO

The proposed JA-STSK and JA-MS-STSK schemes are not restricted to specific multiple-access systems. They may be employed in single-user, multi-user, single-carrier and multi-carrier systems at any carrier frequency. Nevertheless, NOMA schemes are expected to be employed in the next generations of mobile communications systems, hence we

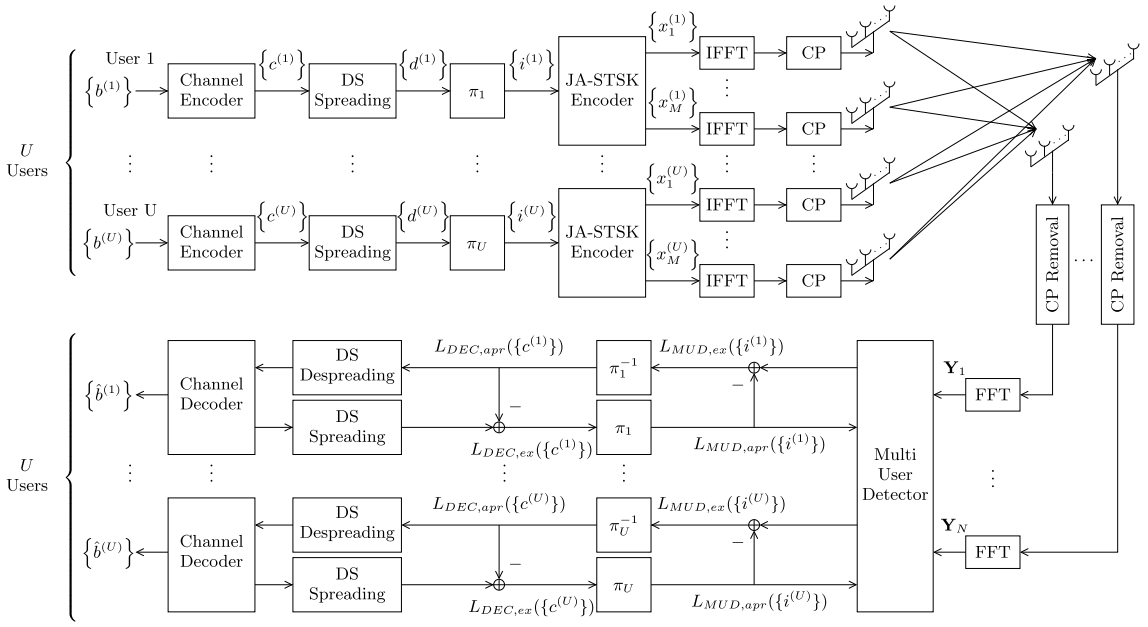


**FIGURE 4.** MC-IDMA uplink communication system's block diagram for JA-STSK supporting $U$ users employing recursive systematic convolutional or irregular convolutional coding and direct sequence spreading as well as iterative, soft-input soft-output MUD at the BS. Multiple antenna arrays, each employing multiple antenna elements, are employed by each user as well as at the BS. When JA-MS-STSK is used, there is a switch to the available AAs at the end of each RF chain.

believe that they provide a compelling application scenario for testing the performance of the proposed MIMO schemes. More specifically, by supporting multiple users in a multi-carrier scenario using channel coding and by allowing them to interfere with each other, the SNR gains achieved by the suggested scheme are expected to be lower, especially when low-complexity suboptimal detectors are employed. As a benefit, an increased system throughput is achieved and the system investigated becomes more realistic than a single-user single-carrier scenario.

The MC-IDMA system depicted in Fig. 4 supports $U$ users. The $u$th user encodes his / her information bit stream $\{b^{(u)}\}$ by using a channel encoder, which in our contribution is assumed to be either a Recursive Systematic Convolutional (RSC) code or an IrCC. The encoded bit stream $\{c^{(u)}\}$ is then spread by using a Direct Sequence (DS) spreader. Since in IDMA each user employs a unique interleaving sequence in order to interleave the spread bits $\{d^{(u)}\}$, it is not detrimental to allocate the same spreading code to each user. Therefore, the repetition code may be used for DS spreading in Fig. 4 with a spreading factor of $SF$. The interleaved bit stream $\{i^{(u)}\}$ is then encoded by the JA-STSK encoder.

Regardless of the MIMO scheme employed, if only single-element antennas were used as in our single-user single-carrier scenarios, the performance of any system would remain modest, due to the high path loss of mm-Wave signals [11]. Hence, we have opted for employing transmit and receive AAs instead, in order to use Analog Beam-Forming (ABF), as depicted in Fig. 4. More specifically, $N_{AA}^t$ and $N_{AA}^r$ antenna elements participate in each transmit and receive AA, respectively, in order to achieve a maximum beamforming gain of $10\log_{10}(N_{AA}^t \cdot N_{AA}^r)$ dB. Furthermore, each antenna element is attached to a pair of phase-shifters and power amplifiers, while each RF chain is connected to a single AA. Therefore, from this point onwards, we assume that the RF chains of the MIMO schemes in Fig. 1, Fig. 2 and Fig. 3 drive AAs instead of single antennas.

Let us assume that each user has the same number of transmit AAs $N_t$ and $M \leq N_t$ RF chains, while the BS is equipped with $N_r$ receive AAs. Similarly to OFDMA, in MC-IDMA we have $M = N_t$, since all transmit AAs have to transmit a signal after the IFFT operation of Fig. 4. On the other hand, as analysed in [7] in the context of MS-STSK, in single carrier systems it is allowed to have more AAs $N_t$ than RF chains $M$ at the transmitter, providing an increased throughput, when these extra antenna combinations are used for conveying more information. This is the reason that JA-MS-STSK may only be used in single-carrier NOMA systems, while JA-STSK may be used in both single-carrier and multi-carrier NOMA systems.[2]

[2]In more detail, in multi-carrier systems it is required for every AA to be connected to an RF chain. This is true because the duration of every information symbol - or STSK codeword - is increased in multi-carrier systems, due to the IFFT operation, resulting in the fact that even though a specific AA would only be active for a short symbol duration in a single-carrier system, that same AA has to be active throughout the transmission of all parallel information symbols that consist an OFDM symbol in multi-carrier systems. Therefore, if an RF chain should be connected at the same time to each of the AAs that would be activated even for a single information symbol in multi-carrier systems. MS-STSK uses fewer RF chains than AAs, therefore this is the reason why it is not suitable for multi-carrier systems. Hence, the same conclusion applies for JA-MS-STSK. On the other hand, the number of RF chains is the same as the number of AAs in JA-STSK, which enables it to be integrated in both single-carrier and multi-carrier systems.

### A. TRANSMISSION AND RECEPTION OVER mm-WAVE CHANNELS

The JA-STSK codeword is then appropriately mapped to the corresponding AAs and then the IFFT operation is performed in order to transform the codewords from the frequency to the time domain. Let us note that each OFDM symbol, which consists of the signals transmitted by all transmit antennas over all subcarriers, includes a different JA-STSK codeword element on each subcarrier, but all these elements correspond to the same time slot. Based on our previous scenario, during the first OFDM symbol, the $N_t = M$ transmit AAs would transmit on each subcarrier elements from the first column of the modulated MS-STSK codeword from the set of (18). In other words, different subcarriers in the same OFDM symbol will transmit the signals corresponding to the same time slot of different JA-STSK codewords, as described in [48]. The following time slot of the same JA-STSK codewords will be transmitted by the same subcarriers in the subsequent OFDM symbol. A cyclic prefix is attached and the signals are transmitted over mm-Wave channels.

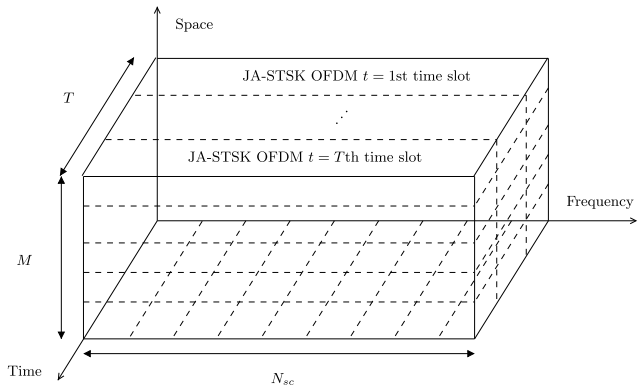


**FIGURE 5.** Mapping of the JA-STSK codewords to the transmitted OFDM symbols.

The JA-STSK codewords are mapped to the $N_{sc}$ number of subcarriers as described in Fig. 5. More specifically, each subcarrier consists of all $M$ rows of the $t$th column of a JA-STSK codeword, where $t = 1, \ldots, T$. The $(t+1)$th column of the same JA-STSK codeword will be transmitted on the same subcarrier at the following OFDM symbol. Therefore, during each OFDM symbol, the $t$th column of $N_{sc}$ number of different JA-STSK codewords is transmitted. The channel is assumed to be constant over $T$ time slots, which can be achieved at mm-Wave frequencies, where the typical channel coherence time is on the order of a few milliseconds, while a single OFDM symbol's duration is a few microseconds.

A mm-Wave channel may be modelled as a time dispersive wideband channel [49]–[51]. Furthermore, the tap delay line model may be used to describe the Channel Impulse Response (CIR) of a mm-Wave channel [52]. Channel models may be classified into physical and analytical models [53]. While an analytical channel model is based on the mathematical formulation of the channel, a physical channel model exploits the electromagnetic characteristics of the transmitted signal. In our contribution, we have used a stochastic physical channel model, which relies on a probabilistic model for creating a Channel's Impulse Response (CIR). Existing probabilistic models for MIMO systems may be adopted for mm-Wave channels by appropriately modifying their main parameters, such as the carrier frequency and the transmission environment, based on practical measurement campaings [49], [50], [54], [55]. The probabilistic model we used for simulating mm-Wave channels in this paper is created based on outdoor urban measurement campaigns conducted at a carrier frequency of 28 GHz [50].

Each transmit AA consists of $N_{AA}^t$ antenna elements, while each receive AA includes $N_{AA}^r$ antenna elements, which are used in order to perform ABF, by appropriately steering the antenna elements of each AA at the users and the base station. The analog beamforming aids in overcoming the high path loss of a mm-Wave system with the assistance of power amplifiers and phase shifters at each transmit and receive AA [8], [13]. More specifically, based on (26), the symbol $x_{n_t,t}^{(u)}$ is allocated to the $n_t$th AA of the $u$th user during the $t$th time slot, for $u \in \{1, 2, \ldots, U\}$, $n_t \in \{1, 2, \ldots, N_t\}$ and $t \in \{1, 2, \ldots, T\}$. Before it is transmitted, ABF is applied to it by a pair of phase-shifters and power amplifiers by multiplying it with a unique ABF coefficient for each antenna element of that AA. In other words, the symbol $x_{n_t,t}^{(u)}$ is multiplied by the complex $(N_{AA}^t \times 1)$-element complex-valued ABF vector $\mathbf{w}_{n_t}^{(u)}$, which satisfies $\mathbf{w}_{n_t}^{(u)} \cdot (\mathbf{w}_{n_t}^{(u)})^H = \mathbf{I}_{N_{AA}^t}$. Similarly, at the $n_r$th AA at the BS, the received signal is multiplied by a $(N_{AA}^r \times 1)$-element complex-valued ABF vector $\mathbf{p}_{n_r}$, where we have $\mathbf{p}_{n_r} \cdot \mathbf{p}_{n_r}^H = \mathbf{I}_{N_{AA}^r}$.

Each user may employ its own JA-STSK codebook. More specifically, at the $v$th level of the $u$th user, with $v = 1, \ldots, V^{(u)}$, there may be $Q_v^{(u)}$ dispersion matrices, $L_v^{(u)}$ symbols of the PSK / QAM symbol constellation and $K_v^{(u)}$ AACs. The resultant number of bits per JA-STSK codeword for the $u$th user is

$$B^{(u)} = \log_2(J) = \log_2\left(\sum_{v=1}^{V^{(u)}} Q_v^{(u)} \cdot L_v^{(u)} \cdot K_v^{(u)}\right). \quad (25)$$

Hence, the $(N_t \times T)$-element JA-STSK codeword $\mathbf{X}^{(u)}$ transmitted by the $u$th user belongs to its associated joint alphabet, as encapsulated in

$$\mathbf{X}^{(u)} = \left\{\mathcal{X}_1^{(u)}, \ldots, \mathcal{X}_V^{(u)}\right\}, \quad (26)$$

where the joint alphabet of the $u$th user is described in (21). In our treatise each user utilizes the same joint alphabet, but this is not obligatory, since each user can adjust its JA-STSK design to fit their own throughput requirements. Therefore, in our simulations we have $\mathbf{X}^{(u)} = \mathbf{X}$, for $u \in \{1, 2, \ldots, U\}$.

At the receiver, after the CP removal, an FFT operation takes place in order to map the received signals back to the frequency domain. Equivalently, we may model the

whole transmission and reception process in the frequency domain, by exploiting the $(N_{AA}^r \cdot N_r \times U \cdot N_t \cdot N_{AA}^t)$-element Frequency Domain CHannel Transfer Function (FD-CHTF) $\mathbf{H}_q$ on the $q$th subcarrier of the mm-Wave channels [14]. As mentioned before, we assume quasi-static channels, which exhibit the same channel states over $T$ time slots. Furthermore, we have assumed that different antenna elements on the same AA experience the same channel, due to the small spacing. Hence, the received signal on the $q$th subcarrier, with $q = 1, 2, \ldots, \mathcal{Q}$ is formulated as

$$\mathbf{Y}_q = \mathbf{P}\mathbf{H}_q\mathbf{W}\tilde{\mathbf{X}}_q + \mathbf{N}_q, \tag{27}$$

where $\mathbf{Y}_q$ is the $(N_r \times T)$-element matrix that includes the received signals, while $\mathbf{P}$ and $\mathbf{W}$ are the $(N_r \times N_{AA}^r \cdot N_r)$-element and $(U \cdot N_t \cdot N_{AA}^t \times U \cdot N_t)$-element diagonal matrices, respectively, that describe the ABF at the BS and the users, respectively, for $T$ time slots. The diagonal ABF matrix $\mathbf{P}$ employs the aforementioned ABF vector $\mathbf{p}_{n_r}$ on its $n_r$th row, while the transmit ABF matrix $\mathbf{W}$ used the ABF vector $\mathbf{w}_{n_t}^{(u)}$ on its $(n_t \cdot U + u)$th column. The $(N_{AA}^r \cdot N_r \times U \cdot N_t \cdot N_{AA}^t)$-element FD-CHTF $\mathbf{H}_q$ consists of the frequency-domain channel states of all users' channels on the $q$th subcarrier and $\mathbf{N}_q$ is the $(N_r \times T)$-element Additive White Gaussian Noise (AWGN) matrix, where each element has zero mean and a variance of $N_0$. Finally, $\tilde{\mathbf{X}}_q = [\mathbf{X}^{(1)}, \ldots, \mathbf{X}^{(U)}]^T$ is the $(N_t \cdot U \times T)$-element symbol matrix that includes the JA-STSK codeword of each user. The transmission power of each user is normalized to unity and we assume a synchronous system, where all signals are added at each AA at the BS.

### B. ITERATIVE DETECTION AND DECODING

Assuming perfect knowledge of the FD-CHTF and the analog beamforming matrices at the BS, the MUD exploits the $N_r$ received signals on a subcarrier basis and provides the $U$ parallel decoder chains of Fig. 4 with their respective bit-based Log Likelihood Ratios (LLR). On the $q$th subcarrier, the extrinsic LLR of the $u$th user's $l$th bit output from the MUD is formulated as

$$L_{MUD,ex}\left(i_l^{(u)}\right) = \ln \frac{\sum_{\hat{\mathbf{X}} \in \chi(u,l,0)} P(\mathbf{Y}_q|\hat{\mathbf{X}})P(\hat{\mathbf{X}})}{\sum_{\hat{\mathbf{X}} \in \chi(u,l,1)} P(\mathbf{Y}_q|\hat{\mathbf{X}})P(\hat{\mathbf{X}})} - L_{MUD,apr}\left(i_l^{(u)}\right), \tag{28}$$

where $\chi(u, l, \mathrm{v})$ is the set of legitimate multi-user JA-STSK codewords, which have the $u$th user's $l$th bit equal to v, with $u \in \{1, 2, \ldots, U\}$, $l \in \{1, 2, \ldots, \log_2 B^{(u)}\}$ and $\mathrm{v} \in \{0, 1\}$. Furthermore, $L_{MUD,apr}(i_l^{(u)})$ is the *a priori* LLR of the $u$th user's $l$th bit, which is initially set to 0, since all bit values are assumed to be equiprobable, while $P(\hat{\mathbf{X}})$ is the *a priori* symbol probability of the multi-user JA-STSK codeword $\hat{\mathbf{X}} = [\mathbf{X}^{(1)}, \ldots, \mathbf{X}^{(U)}]^T$, which is equal to the product of the bit-based *a priori* probabilities. Additionally, $P(\mathbf{Y}_q|\hat{\mathbf{X}})$ is the channel probability and it participates in the MUD's Cost Function (CF), as formulated by [6]

$$f_{CF}(\hat{\mathbf{X}}) = P(\mathbf{Y}_q|\hat{\mathbf{X}})P(\hat{\mathbf{X}}) = \exp\left(-\left\|\mathbf{Y}_q - \mathbf{P}\mathbf{H}_q\mathbf{W}\hat{\mathbf{X}}\right\|^2 / N_0\right) \cdot P(\hat{\mathbf{X}}). \tag{29}$$

The bit-based extrinsic LLRs of each user are then deinterleaved based on their user-specific interleaving sequence and then they are despread, before being fed to the $U$ channel decoders as *a priori* LLRs. The channel decoders of Fig. 4 then generate the bit-based *a posteriori* LLRs for their datawords, as well as their codewords, with the latter being fed back to the DS spreading operation, to the user-based interleavers and eventually to the MUD for further iterations. After a predetermined number of MUD-Despreading/Spreading-DEC iterations $I$, a hard decision is made on the dataword's bit-based LLRs at the output of the channel decoders and each user's information bit estimates are obtained.

## V. GAINS, THROUGHPUT AND COMPLEXITY OF JA-STSK

### A. DIVERSITY GAIN

The diversity gain achieved by JA-STSK is the same as that of STSK and it is equal to

$$\zeta_{DG} = N_r \cdot \min(M, T), \tag{30}$$

where $N_r$ is the receive diversity gain and $\min(M, T)$ is the transmit diversity gain. In our paper, we have opted for $V \leq M - T$ and $D_v \geq T$ for $v = 1, 2, \ldots, V$, if $M \geq T$, in order to maintain the same transmit diversity gain among systems with the same $T$ and different number of RF chains $M$. The presence of multiple independent users and their fair treatment by the MUD and the iterative decoding process jointly determine the system's multiplexing gain of $\zeta_{MG} = U$.

### B. THROUGHPUT

The system's throughput may be formulated as

$$Throughput = \frac{R \cdot B}{T \cdot SF} \text{ (bits per channel use)}, \tag{31}$$

where $B = \sum_{u=1}^{U} B^{(u)}$ is the number of bits per multi-user JA-STSK codeword, $R$ is the coding rate of the channel code selected and it is assumed that all users employ the same coding rate $R$, spreading factor $SF$ and number of time slots $T$ per JA-STSK codeword. The system's DCMC capacity may calculated based on [6], [56]

$$\mathcal{C} = \frac{1}{T}\left(B - \frac{1}{2^B}\sum_{i=1}^{2^B}\mathbb{E}\left[\log_2\left\{\sum_{j=1}^{2^B}\exp\left(\Psi^{(i,j)}\right)\right\}\right]\right), \tag{32}$$

where the MUD, the deinterleavers and the DS despreading processes are assumed to be part of the inner decoder. The expectation operator of (32) is applied over all subcarriers of all OFDM symbols, where we have:

$$\Psi^{(i,j)} = -\frac{\left\|\mathbf{P}\mathbf{H}_q^{(o)}\mathbf{W} + \mathbf{N}_q^{(o)}\right\|^2 + \left\|\mathbf{N}_q^{(o)}\right\|^2}{N_o}, \tag{33}$$

with $\mathbf{H}_q^{(o)}$ and $\mathbf{N}_q^{(o)}$ being the FD-CHTF and noise matrices, respectively, of the $o$th OFDM symbol's $q$th subcarrier, similarly to the respective matrices used in (27).

### C. ONLINE COMPUTATIONAL COMPLEXITY

The multi-user detection complexity imposed during a single iteration of the MAP detector in terms of the number of CF Evaluations (CFE) of (29) per bit is equal to

$$N_{CFEs/bit}^{(MAP)} = \frac{\prod_{u=1}^{U} 2^{B^{(u)}}}{\sum_{u=1}^{U} B^{(u)}} \text{ (CFEs / bit)}, \tag{34}$$

where $B^{(u)}$ is the number of bits per JA-STSK codeword employed by the $u$th user. Furthermore, due to their employment in the size of all matrices in (29), the number of users $U$ as well as both the number of transmit and receive AAs $N_t$ and $N_r$, respectively, affect the computational complexity, since they determine the number of associated Add-Compare-Select (ACS) operations required for each CFE. The number of RF chains $M$ determines the sparsity of those matrices therefore, it also influences the computational complexity.

The HIHO and SISO QMUDs employed impose a complexity on the order of $O\left(\sqrt{N_{CFEs/bit}^{(MAP)}}\right)$, as investigated in [26], and [43]–[45]. Please note that in the HIHO QMUD we only search for the single most likely multi-user JA-STSK codeword, while in the SISO QMUD a subset of the most probable multi-user JA-STSK codewords is required for creating the LLRs, therefore we always have $N_{CFEs/bit}^{(HIHO-QMUD)} < N_{CFEs/bit}^{(SISO-QMUD)}$.

It should be noted that the computational complexity of the hard-output ML detectors of (5), (13) and (23), quantified in terms of the number of CFEs / bit depends on the size of the legitimate codeword alphabet. For a fair comparison between STSK, JA-STSK, MS-STSK and JA-MS-STSK, the throughput of the system should be the same, regardless of the MIMO scheme employed. Based on (31), this means that the number of bits per codeword $B$ should be the same in all MIMO schemes. Therefore, the number of STSK, JA-STSK, MS-STSK and JA-MS-STSK codewords should also be the same in both schemes and equal to $2^B$. Hence, when two systems employ different MIMO schemes, but have the same throughput and employ the same detector at the receiver, the computational complexity of the detector should require the same number of CFEs.

However, the complexity of each CFE may differ between the systems. Let us focus on the single-user single-carrier scenarios of (5), (13) and (23), where an ML detector is used. Similar conclusions may be readily drawn for multi-user multi-carrier systems employing iterative detectors. The number of ACS operations per CFE in each system depends on the number of receive antennas $N_r$, the number of time slots $T$, the number of RF chains at the transmitter $M$, the number of transmit antennas and, in the case of JA-STSK and JA-MS-STSK, the number of alphabet levels $V$. In other words, the computational complexity of a single CFE at the receiver's detector depends on the size and the sparsity of the legitimate codewords. Given that the expensive resource of $M$ RF chains is kept the same between an STSK and MS-STSK system, the MS-STSK system will employ more transmit antennas $N_t^{(MS-STSK)} > N_t^{(STSK)}$, while reducing the number of dispersion matrices $Q^{(MS-STSK)} < Q^{(STSK)}$ and the constellation size $L^{(MS-STSK)} < L^{(STSK)}$. Since among these three values only the number of transmit antennas affects the number of ACS operations at the detector, an MS-STSK system is expected to require a higher number of ACS operations per CFE than an STSK system. In the JA-STSK scheme both the number of RF chains and that of the transmit antennas remains the same as that of its counterpart, formulated as $M^{(JA-STSK)} = M^{(STSK)}$ and $N_t^{(JA-STSK)} = N_t^{(STSK)}$, respectively. The gain is achieved by using a subset of the available RF chains in conjunction with different dispersion matrices and constellation sizes per level. Hence, the number of ACS operations per CFE at the detector of the JA-STSK scheme is the same as that at the detector of the STSK scheme. On the other hand, the JA-MS-STSK scheme requires the same number of ACS operations as the MS-STSK scheme, again, given that the number of RF chains and transmit antennas are the same for the two schemes.

### D. HARDWARE COMPLEXITY

However, the *hardware* complexity required by the MS-STSK, JA-STSK and JA-MS-STSK in single-carrier systems is higher than that required at the STSK, even if the number of RF chains and number of transmit antennas is kept the same, since a switch is required for connecting the RF chains to the specific transmit antennas that should be activated for each codeword. In multi-carrier systems, where every antenna should be activated regardless of the selected antenna combination, no additional hardware complexity is imposed on the proposed JA-STSK scheme.

### E. OFFLINE COMPUTATIONAL COMPLEXITY

The creation of the joint alphabet in JA-STSK and JA-MS-STSK may be performed off-line, but naturally, both the transmitter and the receiver should be aware of the resultant codebook. The optimization of the joint alphabet is a separate problem that may also be performed off-line. The off-line complexity of creating optimal alphabets for the JA-STSK is determined by the selection of the optimal combination of dispersion matrices, constellations and antenna combinations. That off-line complexity is expected to be higher than that required for the creation of the STSK codewords, which mainly focuses on the generation of the optimal dispersion matrices for each symbol constellation.

## VI. FAIR ANTENNA ARRAY SELECTION

The methodology followed by the proposed JA-STSK for AA selection is important in terms of the achievable capacity and performance of the system. Since each alphabet uses a

unique number of RF chains, the specific RF chain indices that participate in each AAC directly affect the correlation between the JA-STSK codewords when the same AAs are activated in two or more AACs, similarly to the MS-STSK scheme [7]. In MS-STSK, a fixed number $M$ of RF chains participates in each AAC, when the number of available AAs $N_t$ is higher than the number of RF chains $M$. For example, given a system having $N_t = M = 4$ antennas, the indices of $\{1, 2, 3, 4\}$ are available. Then, assuming that a pair of AACs is required, where two out of the $N_t = 4$ AAs will be used in each AAC, then the specific pair of AACs $\{[1, 2], [3, 4]\}$ will result in a lower JA-STSK codeword correlation than the pair of AACs $\{[1, 2], [1, 3]\}$, since the latter uses the first AA in both AACs, essentially increasing the correlation of the potentially received signals by the two different AA pairs.

In other words, in order to achieve the lowest possible correlation between the AACs, the number of AACs that each AA participates in should approximate a uniform distribution. That way each AA will offer a similar average performance, when transmitting over the quasi-static channel. Therefore, the correlation between the JA-STSK codewords will be minimized, when generating the joint alphabet. Since a joint alphabet is formed in JA-STSK, we have opted for computing the antenna combinations based on an algorithm that only depends on the number $K_v$ of AACs per level, for $v = 1, 2, \ldots, V$, instead of separately generating the AACs for each level. By using this multi-level AA selection method, we may treat the AAs in a fair manner.

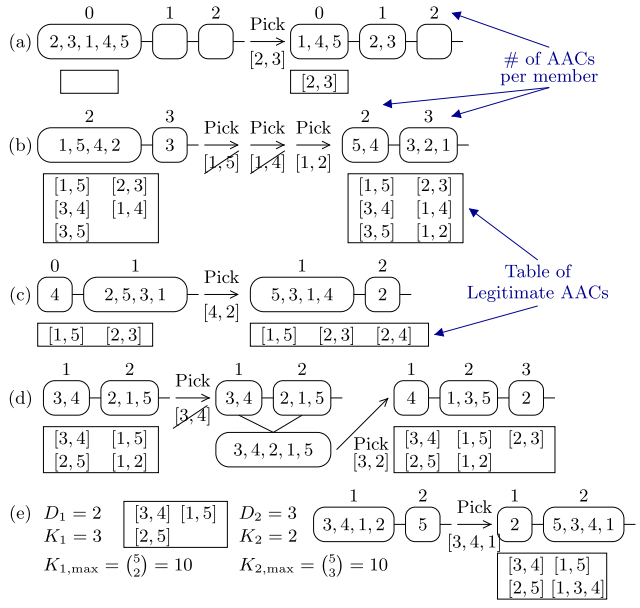


**FIGURE 6. Characteristic examples of the proposed fair AAC selection methodology. In these examples, there are $N_t = M = 5$ RF chains and $D_1 = 2$ RF chains participate in each AAC in (a), (b), (c) and (d).**

Examples of the AA selection methodology are portrayed in Fig. 6. The fair AA selection algorithm creates and updates the pools of AAs in a pseudo-random fashion, based on the number of AACs they are already participating in. Initially, all the AAs belong to the first pool, which corresponds to 0 AACs, since none of them has been used yet. Starting from the specific level that activates the lowest number $D_1$ of AAs, without any loss of generality, we scramble the order of appearance of the AAs in that pool using a random interleaver, as in Fig. 6a. Then we select the first AAC as in Fig. 6a. The newly formed AAC is first checked against the existing AACs of that specific level, which are stored in an array in memory. If the newly formed AAC is unique, it is stored in the same array and at the same time, the selected AAs move to the next pool, which corresponds to an additional AAC, as depicted in Fig. 6a and Fig. 6b. Otherwise, if the newly formed AAC is a duplicate, the next AAC is chosen, as if counting backwards in the binary domain, as shown in Fig. 6b. We always proceed by picking an AAC from the non-empty pool that corresponds to the fewest AACs. If that pool includes fewer AAs than the ones required by the AAC of that level, then all of them are selected and the remaining AAs are picked from the next non-empty pool, as in Fig. 6c. Furthermore, in the case where all combinations in a pool have already been generated, an auxiliary pool is created by combining that pool and the next pool, in that order, and the same selection procedure is repeated, as illustrated in Fig. 6d. After an AAC is found, the auxiliary pool returns the AAs to their respective updated pools. When the AACs of a level have been generated, the pools remain the same, but the AACs required for the subsequent level are now generated, as seen in Fig. 6e. This procedure continues, until all AACs have been stored in the array. The proposed pseudo-random algorithm was designed so that for the predetermined interleaving sequences per level, both the transmitters and the receiver are able to generate the same legitimate AACs, eliminating the requirements of opting for a random selection of AACs.

## VII. SIMULATION RESULTS

Let us now investigate both MC-IDMA and SC-IDMA systems, supporting multiple users with the aid of the newly defined JA-STSK($N_t, N_r, T, \mathbf{Q}, \mathbf{L}, \mathbf{K}$) and the JA-MS-STSK($N_t, M, N_r, T, \mathbf{Q}, \mathbf{L}, \mathbf{K}$) schemes, respectively,[3] comparing their performance to that of the STSK($N_t, N_r, T, Q, L$) scheme. Table 5 summarizes the system parameters that are used in the simulations. In single-carrier scenarios we employ a single antenna element per transmit and receive AA, while a pair of antenna elements is used in each AA of mm-Wave multi-carrier systems in order to benefit from the ABF applied by each of the AA selected in the mm-Wave IDMA system. In our contribution we have made the simiplifying assumption that each user has the same distance from the BS and experiences similar channel conditions. Therefore,

[3]In our simulations, the values of the number of dispersion matrices per level and the symbol constellation's size per level included in $\mathbf{Q}$ and $\mathbf{L}$, respectively, were found heuristically based on their resultant associated BER performance. An optimal method for selecting the specific symbol constellations' size $\mathbf{L}$, the number of dispersion matrices $\mathbf{Q}$, as well as the actual dispersion matrices $\mathbf{A}_{v,q}$ is a topic for future research.

**TABLE 5. Parameters of the investigated scenarios.**

| | |
|---|---|
| No. of Users | $U = 1, 2, 3$ |
| No. of RF chains per User | $M = 5$ |
| No. of AAs at each User | $N_t = 5$ (MC-IDMA) |
| | $N_t = 10$ (SC-IDMA) |
| No. of AAs at Receiver | $N_r = 5$ |
| No. of antenna elements at each AA | $N^t_{AA} = N^r_{AA} = 2$ (MC-IDMA) |
| | $N^t_{AA} = N^r_{AA} = 1$ (SC-IDMA) |
| No. of Time Slots | $T = 2$ |
| Normalized Load | $U_L = U \cdot M/N_r = 1, 2, 3$ |
| Joint Symbol Constellation | $\mathbf{L} = [L_1, L_2, L_3, L_4, L_5]$ |
| Symbol Constellation per Level | $L_v = 0, 2, 4, 8$ |
| Joint Dispersion Matrices | $\mathbf{Q} = [Q_1, Q_2, Q_3, Q_4, Q_5]$ |
| No. of Dispersion Matrices per Level | $Q_v = 0, 2, 4, 8$ |
| Joint AACs | $\mathbf{K} = [K_1, K_2, K_3, K_4, K_5]$ |
| No. of AACs per Level | $K_v = 0, 1, 2, 3, 4$ |
| No. of AAs per AAC per Level | $D_v = [1, 2, 3, 4, 5]$ |
| Spreading Factor | $SF = 2$ |
| Channel Model (MC-IDMA) | mm-Wave |
| Channel Model (SC-IDMA) | Non-Dispersive Rayleigh |
| Carrier Frequency | $f_c = 28$ GHz (MC-IDMA) |
| | $f_c = 2.5$ GHz (SC-IDMA) |
| Sampling Frequency | $f_s = 500$ MHz (MC-IDMA) |
| | $f_s = 15.36$ MHz (SC-IDMA) |
| Number of Subcarriers (MC-IDMA) | $\mathcal{Q} = 1024$ |
| Cyclic Prefix | CP = 100 |
| Frame Length | 1024 STSK codewords per user |

the same transmission power has been allocated to each of the users.

Figure 7 presents the throughput gain attained when JA-MS-STSK replaces STSK in a $U = 2$-user SC-IDMA system, as a function of the hardware complexity, defined in terms of the number of additional antenna arrays at each user, as well as versus the computational complexity, represented by the number of CFEs in (29) at the BS. The proposed fair AAC selection algorithm was used in all JA-MS-STSK scenarios. We may observe that even without requiring additional transmit antenna arrays, the proposed JA-MS-STSK results in a throughput gain, which is determined both by the system's dimensionality and by the SNR. As we increase the number of transmit antenna elements, the gain of all systems is increased. To elaborate, the gain gradient decreases, but still remains positive for a specific multi-user system, because we opted for keeping the same [**Q**, **L**, **K**] configuration, regardless of the number of transmit antenna arrays. By carefully optimizing each system for different $N_t$, we expect to exhibit higher gains. Moreover, the gain demonstrated by the system, where $B = 14$ bits per multi-user codeword are used, is lower than that of $B = 12$, due to the operation at $SNR = 2$ dB per receive antenna array, which is the SNR value at which the $B = 12$-system associated with JA-MS-STSK approaches its maximum gain.

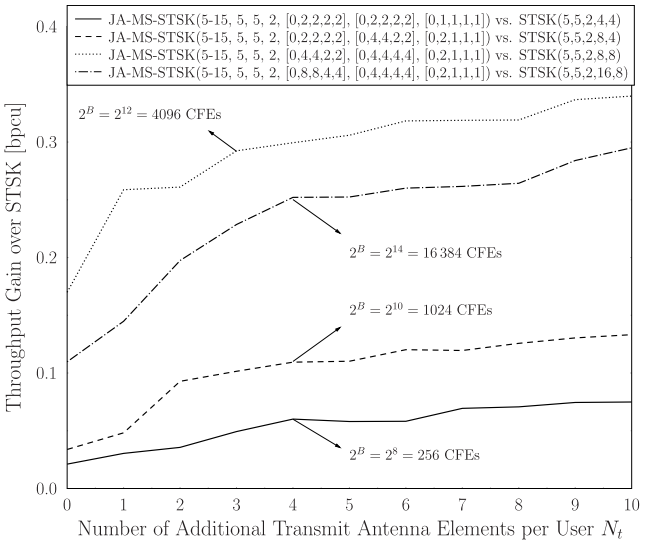


**FIGURE 7. Throughput gain for JA-MS-STSK schemes over STSK schemes with the same maximum throughput in a $U = 2$-user SC-IDMA system at SNR = 2 dB.**

At the current state of the art there are no mathematical tools that can analyse the performance of iterative receiver schemes. Hence the powerful semi-analytical tool of EXIT charts was invented by ten Brink [46], [57] for representing the exchange of mutual information between the component detectors and decoders. The output of the receiver has to be Gaussian distributed, which can be approximated with the aid of long interleavers [46]. In the absence of this condition we can use a histogram based EXIT chart analysis [6]. In the extreme case of short interleaver schemes we have to use EXIT-band charts. These techniques are well established and widely accepted in the communications community. To elaborate a little further, the beneficial insights provided by the EXIT chart are as follows:

1) The area under the inner decoder's EXIT curve quantifies the achievable throughput.
2) The area between the inner and outer decoders' EXIT curves is proportional to the distance from the achievable throughput.
3) The area under the outer decoder's EXIT curve quantifies the code-rate.

For further details, please refer to [6] and [46] . It remains an open challenge for the research community to find true analytical insights concerning the performance of iterative detection aided systems in general and for STSK in particular.

Figure 8 presents the EXIT chart of a $U = 2$-user MC-IDMA system when the output Mutual Information (MI) of the MUD is represented as the inner decoder and the despreading / channel decoding operations form the outer decoder. We may observe that the JA-STSK(5, 5, 2, [0, 2, 2, 2, 2], [0, 4, 4, 2, 2], [0, 2, 2, 1, 1]) scheme employing the proposed fair AA selection attains a higher achievable rate than the STSK(5, 5, 2, 8, 8) scheme, especially in the high coding rate region. Even though the

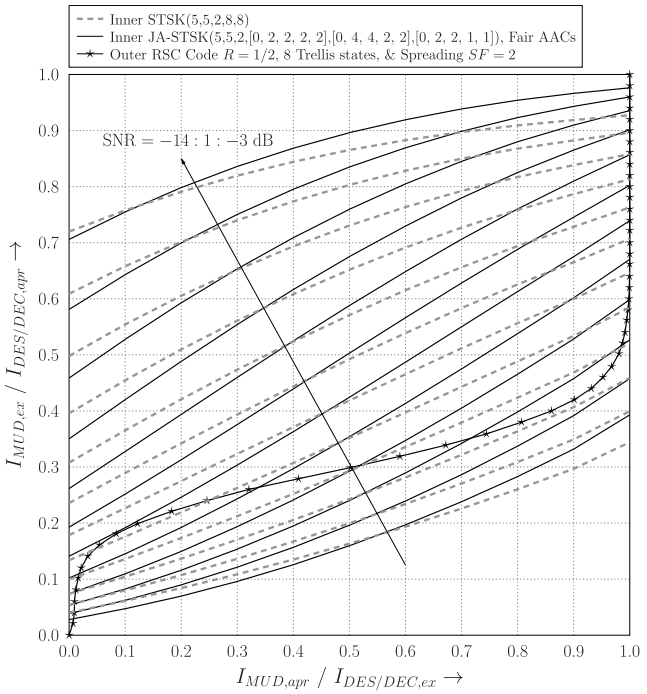


**FIGURE 8.** EXIT chart of an MC-IDMA system supporting $U = 2$-users, where the STSK and JA-STSK schemes are used as the inner decoder for various values of SNR per receive AA. The outer decoder incorporates an RSC code with $R = 1/2$ and 8 Trellis states, along with a spreading code of $SF = 2$, resulting in a joint coding rate of $R/SF = 0.25$.

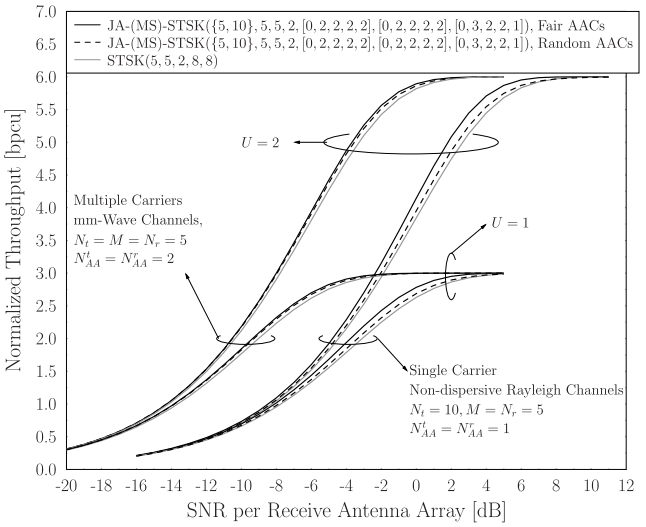


**FIGURE 9.** Normalized throughput with respect to SNR per receive AA for MC-IDMA and SC-IDMA systems, when the JA-STSK and JA-MS-STSK schemes are used, respectively. The performance of the fair AAC selection algorithm is compared to that of the random AAC selection. The performance of the STSK scheme is included as benchmark.

capacity gain is modest, it should be noted that it comes without any cost for the JA-STSK in MC-IDMA systems, since no additional hardware or decoding complexity is required. The only additional process compared to an STSK system is in the generation of the joint alphabet, which may be carried out offline both at the users and at the BS's receiver by using the fair AA selection algorithm in conjunction with predetermined interleavers, as mentioned in Section VI.

For a joint spreading and coding rate target of $R/SF = 0.25$ associated with $SF = 2$ and $R = 1/2$, the minimum required SNR per receive AA is $-11.9$ dB for JA-STSK and $-12.1$ dB for STSK. By using an RSC code having $R = 1/2$ and 8 Trellis states, along with a repetition code used as spreading associated with $SF = 2$, the minimum SNR per receive AA, where we may achieve near-error-free reception, given that sufficient MUD-DES / DEC iterations are affordable, is $-9$ dB for JA-STSK and $-9.6$ dB for STSK, as illustrated in Fig. 8. The loss exhibited by JA-STSK is related to the fact that its initial output MI for $I_{MUD,apr} = 0$ is lower than that of the STSK, hence a higher SNR is required for having an open tunnel. Thus, when combined with an outer code that reaches the $I_{DES/DEC,ex} = 1$ line at relatively low $I_{DES/DEC,apr}$ values, as in the case of the RSC employed in Fig. 8, the STSK provides a lower distance from its achievable capacity. This fact, in conjunction with the higher achievable rate of the JA-STSK, suggests that the potential employment of an IRCC design would benefit JA-STSK more substantially than STSK, yielding a higher rate.

In Fig. 9 we have plotted the normalized throughput of a single-carrier system supporting $U = 1$ or 2 users transmitting over non-dispersive Rayleigh channels, as well as the throughput of a multi-carrier system, where $U = 1$ or 2 users transmit over mm-Wave channels. When transmitting over the mm-Wave channels, each transmit and receive AA includes $N_{AA}^t = N_{AA}^r = 2$ antenna elements, which are used for analog beamforming, leading to the ∼6 dB gain exhibited in Fig. 9. Furthermore, the users of the single-carrier system are equipped with $N_t = 10$ AAs, while all systems include $M = 5$ RF chains per user and $N_r = 5$ receive AAs at the BS. The JA-(MS)-STSK schemes using our fair AAC selection always outperform the same schemes relying on random AACs. At the same time, both the JA-STSK and JA-MS-STSK schemes achieve a higher throughput than STSK, even when random AACs are used in both multi-carrier and single-carrier scenarios. As expected, the throughput gain is higher in the single-carrier scenario, since more transmit AAs are used, hence allowing our fair AAC selection algorithm to uniformly distribute the load across more antennas, hence decreasing the number of AACs that each AA participates in and therefore reducing the correlation between the different JA-MS-STSK codewords.

In order to characterize the capabilities of the SISO QMUDs of [26] in the context of irregular designs, in Fig. 10 we investigate a $U = 3$-user MC-IDMA system having a spreading factor of $SF = 2$, where a suitable IRCC associated with $R = 0.8$ and 32 Trellis states has been found in order to create a narrow but open EXIT tunnel between the Dürr-Høyer Algorithm-aided MUlti-input Approximation with Forward and Backward Knowledge Transfer (DHA-MUA-FBKT) QMUD's inner EXIT curve [26] and the joint outer EXIT curve. The

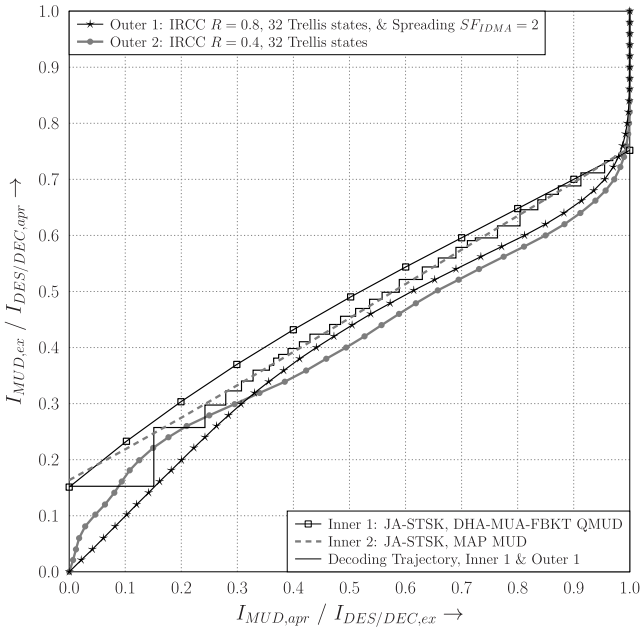


**FIGURE 10.** EXIT chart of an MC-IDMA system supporting $U = 3$ users with 5 bits per JA-STSK(5, 5, 2, [0, 2, 2, 2, 2], [0, 4, 4, 2, 2], [0, 2, 1, 1, 1]) codeword. The inner decoder uses the MAP MUD or the DHA-MUA-FBKT QMUD of [26]. When spreading is used with $SF = 2$, a suitable IRCC with $R = 0.8$ is found for allowing a narrow tunnel between the DHA-MUA-FBKT QMUD and the despreader / decoder in the MC-IDMA system. When no spreading is used, only an IRRC with $R = 0.4$ is used, resulting in a OFDMA system, where all users transmit on all subcarriers. The decoding trajectory corresponds to the MC-IDMA system using the QMUD.

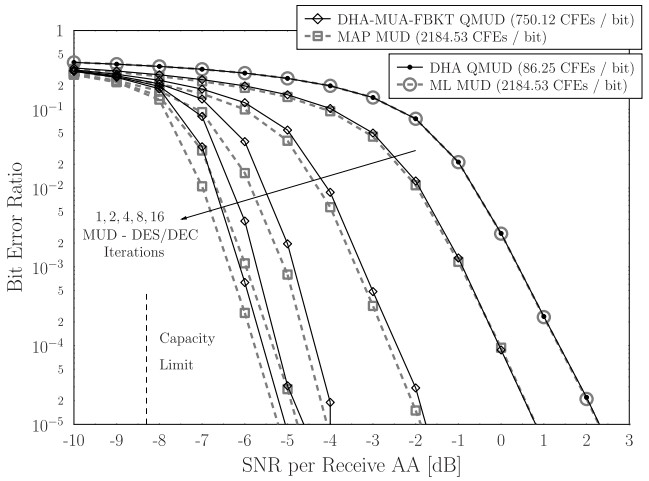


**FIGURE 11.** BER performance versus SNR per receive AA for an MC-IDMA system supporting 3 users with 5 bits per JA-STSK(5, 5, 2, [0, 2, 2, 2, 2], [0, 4, 4, 2, 2], [0, 2, 1, 1, 1]) codeword. The IRCC with $R = 0.8$ and 32 Trellis states of Fig. 10 is employed, along with a spreading factor of $SF = 2$. The HIHO DHA QMUD is compared to the optimal HIHO ML MUD, while the SISO DHA-MUA-FBKT QMUD is contrasted with the optimal SISO MAP MUD for various number of MUD - DES / DEC iterations.

JA-STSK(5, 5, 2, [0, 2, 2, 2, 2], [0, 4, 4, 2, 2], [0, 2, 1, 1, 1]) scheme is used, resulting in 5 bits per JA-STSK codeword per user, or, in other words, $2^{5 \cdot 3} = 32\,768$ legitimate multi-user JA-STSK codewords, which results in a computational complexity of 2184.53 CFEs per bit. At the same time, the QMUD employed requires only 750.12 CFEs per bit, while achieving near-optimal performance.

According to [26], the inner decoder EXIT curve of the DHA-MUA-FBKT QMUD may overshoot that of the optimal MAP MUD for $0 < I_{MUD,apr} < 1$ due to assuming Gaussian distributed input *a priori* LLRs, which in practice follow a different distribution. Since the decoding trajectory has to freely traverse through an open tunnel, regardless of the accuracy of the inner decoder's EXIT curve, our proposed design is now focused on finding an IRCC, which matches the straight line that connects the $[0, I_{QMUD,ex}]$ and $[1, I_{QMUD,ex}]$ points, as seen in Fig. 10. The outer decoder's EXIT curve generated by an IRCC found with the aid of this methodology is expected to also match the MAP MUD's inner decoder EXIT curve.

Both outer decoder EXIT curves of Fig. 10 are associated with a rate of $R/SF = 0.4$ and they use different independently generated IRCCs. The outer decoder's EXIT curve that relies on spreading using $SF = 2$ corresponds to the MC-IDMA system investigated, while the one that has no spreading may be deemed to represent OFDMA, where all users transmit on all available subcarriers. We may conclude from Fig. 10 that MC-IDMA is beneficial in systems where the inner decoder's EXIT curve has a higher gradient, as is the case when user-based Unity Rate Codes (URC) are employed between the MUD and the despreaders / channel decoders, since the outer decoder's EXIT curve associated with low MI is dominated by the despreading operation. Furthermore, the computational complexity of the despreading / channel decoding in MC-IDMA is lower than that of the channel decoding operation in an OFDMA system employing the same joint spreading and coding rate. The decoding trajectory relying on iterating between the SISO QMUD and the despreader / IRCC decoder of the MC-IDMA system in Fig. 10 passes through the open EXIT tunnel and converges at $I_{DES/DEC,ex} = 0.98$ after 40 QMUD-DES/DEC iterations at $SNR = -7.5$ dB, resulting in a a vanishingly low BER. The BER is expected to be infinitesimally low at SNR $= -6.46$ dB, where the inner and outer decoder EXIT curves meet at $I_{MUD,ex} = 0.82$, when $I_{DES/DEC,ex} = 1$.

The BER performance of the $U = 3$-user MC-IDMA system presented in Fig. 10 is depicted in Fig. 11. The DHA QMUD achieves a near-optimal BER performance, approaching that of the ML MUD, while requiring only 3.95% of the ML MUD's complexity, when quantified in terms of the number of CFEs per bit. In terms of absolute numbers this is translated in 86.25 CFEs per bit for the DHA QMUD and 2184.53 CFEs per bit for the ML MUD. By employing the SISO DHA-MUA-FBKT QMUD in the same system we achieve a near-optimal performance, regardless of the number of MUD - DES/DEC iterations for 34.34% of the MAP MUD's complexity. As we increase the number of decoding iterations, we approach the achievable capacity, albeit naturally at the cost of investing more decoding complexity. After 16 decoding iterations, we are 3.08 dB away

from capacity at a BER of $10^{-5}$, partly due to the limited interleaver length of 2048 bits per user and partly because the outer code does not reach the $I_{DES/DEC,ex} = 1$ line in Fig. 10 before an SNR of $-6.46$ dB per receive AA.

## VIII. CONCLUSIONS

In this treatise we showed that the proposed JA-STSK and JA-MS-STSK schemes may replace STSK in MC-IDMA and SC-IDMA, respectively, since they offer a throughput gain, even when no additional complexity is required, as seen in Fig. 7 and Fig. 8. Furthermore, we argued that when our fair AA selection algorithm is used for JA-STSK and JA-MS-STSK, a higher throughput gain is achieved than that offered by a random AA selection algorithm, as evidenced by Fig. 9. In Fig. 10, we demonstrated that MC-IDMA may be beneficially combined with IRCC, since both schemes offer a coding rate flexibility at a moderate decoding complexity, as well as an increased throughput, when compared to orthogonal multiple access schemes. We also presented a design methodology for amalgamating SISO QMUDs with IRCCs. The potential use of QMUDs will reduce the computational complexity quantified in terms of CFEs even further, while achieving a near-optimal performance, as evidenced by their BER performance seen in Fig. 11.

There are numerous of open research topics on JA-STSK and MC-IDMA, which would pave the way for the future systems. A joint dispersion matrix optimization, which would replace the individual level-based optimization that was adopted in this paper, inspired by the procedure followed in STSK [4]–[6], would further increase the system's achievable capacity. Furthermore, designing an algorithm that would optimally allocate the number of dispersion matrices, the constellation size and the number of antenna combinations per level, depending on the maximum or current number of users supported by the system would also be beneficial.

## ACKNOWLEDGEMENT

The use of the IRIDIS High Performance Computing Facility at the University of Southampton is also acknowledged.

## REFERENCES

[1] S. Yang and L. Hanzo, "Fifty years of MIMO detection: The road to large-scale MIMOs," *IEEE Commun. Surveys Tuts.*, vol. 17, no. 4, pp. 1941–1988, 4th Quart. 2015.

[2] C. Xu, S. Sugiura, S. X. Ng, P. Zhang, L. Wang, and L. Hanzo, "Two decades of MIMO design tradeoffs and reduced-complexity MIMO detection in near-capacity systems," *IEEE Access*, to be published.

[3] R. Y. Mesleh, H. Haas, S. Sinanovic, C. W. Ahn, and S. Yun, "Spatial modulation," *IEEE Trans. Veh. Technol.*, vol. 57, no. 4, pp. 2228–2241, Jul. 2008.

[4] S. Sugiura, S. Chen, and L. Hanzo, "Space-time shift keying: A unified MIMO architecture," in *Proc. IEEE Global Telecommun. Conf.*, Dec. 2010, pp. 1–5.

[5] S. Sugiura, S. Chen, and L. Hanzo, "Coherent and differential space-time shift keying: A dispersion matrix approach," *IEEE Trans. Commun.*, vol. 58, no. 11, pp. 3219–3230, Nov. 2010.

[6] L. Hanzo, T. H. Liew, B. Yeap, R. Y. S. Tee, and S. X. Ng, *Turbo Coding, Turbo Equalisation and Space-Time Coding: EXIT-Chart Aided Near-Capacity Designs for Wireless Channels*. Hoboken, NJ, USA: Wiley, 2010.

[7] I. A. Hemadeh, M. El-Hajjar, S. Won, and L. Hanzo, "Multi-set space-time shift-keying with reduced detection complexity," *IEEE Access*, vol. 4, pp. 4234–4246, 2016.

[8] I. A. Hemadeh, P. Botsinis, M. El-Hajjar, S. H. Won, and L. Hanzo, "Reduced-RF-chain aided soft-decision multi-set steered space-time shift-keying for millimeter-wave communications," *IEEE Access*, vol. 5, pp. 7223–7243, 2017.

[9] F. Khan and Z. Pi, "mmWave mobile broadband (MMB): Unleashing the 3–300GHz spectrum," in *Proc. 34th IEEE Sarnoff Symp.*, May 2011, pp. 1–6.

[10] Z. Pi and F. Khan, "System design and network architecture for a millimeter-wave mobile broadband (MMB) system," in *Proc. 34th IEEE Sarnoff Symp.*, May 2011, pp. 1–6.

[11] T. S. Rappaport *et al.*, "Millimeter wave mobile communications for 5G cellular: It will work!" *IEEE Access*, vol. 1, pp. 335–349, May 2013.

[12] W. Roh *et al.*, "Millimeter-wave beamforming as an enabling technology for 5G cellular communications: Theoretical feasibility and prototype results," *IEEE Commun. Mag.*, vol. 52, no. 2, pp. 106–113, Feb. 2014.

[13] I. A. Hemadeh, M. El-Hajjar, S. Won, and L. Hanzo, "Layered multi-group steered space-time shift-keying for millimeter-wave communications," *IEEE Access*, vol. 4, pp. 3708–3718, 2016.

[14] L. Hanzo, O. Alamri, M. El-Hajjar, and N. Wu, *Near-Capacity Multi-Functional MIMO Systems: Sphere-Packing, Iterative Detection and Cooperation*. Hoboken, NJ, USA: Wiley, May 2009.

[15] Y. Saito, Y. Kishiyama, A. Benjebbour, T. Nakamura, A. Li, and K. Higuchi, "Non-orthogonal multiple access (NOMA) for cellular future radio access," in *Proc. 77th IEEE VTC-Spring*, Dresden, Germany, Jun. 2013, pp. 1–5.

[16] Z. Ding, Z. Yang, P. Fan, and H. V. Poor, "On the performance of non-orthogonal multiple access in 5G systems with randomly deployed users," *IEEE Signal Process. Lett.*, vol. 21, no. 12, pp. 1501–1505, Dec. 2014.

[17] L. Dai, B. Wang, Y. Yuan, S. Han, C. L. I, and Z. Wang, "Non-orthogonal multiple access for 5G: Solutions, challenges, opportunities, and future research trends," *IEEE Commun. Mag.*, vol. 53, no. 9, pp. 74–81, Sep. 2015.

[18] Z. Yang, Z. Ding, P. Fan, and G. K. Karagiannidis, "On the performance of non-orthogonal multiple access systems with partial channel information," *IEEE Trans. Commun.*, vol. 64, no. 2, pp. 654–667, Feb. 2016.

[19] Z. Ding *et al.*, "Application of non-orthogonal multiple access in LTE and 5G networks," *IEEE Commun. Mag.*, vol. 55, no. 2, pp. 185–191, Feb. 2017.

[20] Z. Ding, P. Fan, and H. V. Poor, "Random beamforming in millimeter-wave NOMA networks," *IEEE Access*, vol. 5, pp. 7667–7681, 2017.

[21] L. Ping, "Interleave-division multiple access and chip-by-chip iterative multi-user detection," *IEEE Commun. Mag.*, vol. 43, no. 6, pp. S19–S23, Jun. 2005.

[22] L. Ping, L. Liu, K. Wu, and W. K. Leung, "Interleave division multiple-access," *IEEE Trans. Wireless Commun.*, vol. 5, no. 4, pp. 938–947, Apr. 2006.

[23] R. Zhang and L. Hanzo, "Three design aspects of multicarrier interleave division multiple access," *IEEE Trans. Veh. Technol.*, vol. 57, no. 6, pp. 3607–3617, Nov. 2008.

[24] R. Zhang, L. Xu, S. Chen, and L. Hanzo, "EXIT-chart-aided hybrid multiuser detector for multicarrier interleave-division multiple access," *IEEE Trans. Veh. Technol.*, vol. 59, no. 3, pp. 1563–1567, Mar. 2010.

[25] J. Dang, W. Zhang, L. Yang, and Z. Zhang, "OFDM-IDMA with user grouping," *IEEE Trans. Commun.*, vol. 61, no. 5, pp. 1947–1955, May 2013.

[26] P. Botsinis, D. Alanis, Z. Babar, S. X. Ng, and L. Hanzo, "Iterative quantum-assisted multi-user detection for multi-carrier interleave division multiple access systems," *IEEE Trans. Commun.*, vol. 63, no. 10, pp. 3713–3727, Oct. 2015.

[27] Y. A. Chau and S.-H. Yu, "Space modulation on wireless fading channels," in *Proc. IEEE Veh. Technol. Conf.*, vol. 3. Oct. 2001, pp. 1668–1671.

[28] S. Song, Y. Yang, Q. Xionq, K. Xie, B.-J. Jeong, and B. Jiao, "A channel hopping technique I: Theoretical studies on band efficiency and capacity," in *Proc. IEEE Int. Conf. Commun., Circuits Syst.*, vol. 1. Jun. 2004, pp. 229–233.

[29] C. Xu, S. Sugiura, S. X. Ng, and L. Hanzo, "Spatial modulation and space-time shift keying: Optimal performance at a reduced detection complexity," *IEEE Trans. Commun.*, vol. 61, no. 1, pp. 206–216, Jan. 2013.

[30] D. A. Basnayaka and H. Haas, "MIMO interference channel between spatial multiplexing and spatial modulation," *IEEE Trans. Commun.*, vol. 64, no. 8, pp. 3369–3381, Aug. 2016.
[31] J. Jeganathan, A. Ghrayeb, and L. Szczecinski, "Spatial modulation: Optimal detection and performance analysis," *IEEE Commun. Lett.*, vol. 12, no. 8, pp. 545–547, Aug. 2008.
[32] J. Jeganathan, A. Ghrayeb, L. Szczecinski, and A. Ceron, "Space shift keying modulation for MIMO channels," *IEEE Trans. Wireless Commun.*, vol. 8, no. 7, pp. 3692–3703, Jul. 2009.
[33] S. Ganesan, R. Mesleh, H. Ho, C. W. Ahn, and S. Yun, "On the performance of spatial modulation OFDM," in *Proc. Asilomar Conf. Signals, Syst. Comput.*, pp. 1825–1829, Oct. 2006.
[34] R. Abu-alhiga and H. Haas, "Subcarrier-index modulation OFDM," in *Proc. IEEE Int. Symp. Pers., Indoor, Mobile Radio Commun.*, Sep. 2009, pp. 177–181.
[35] S. Sugiura and L. Hanzo, "Single-RF spatial modulation requires single-carrier transmission: Frequency-domain turbo equalization for dispersive channels," *IEEE Trans. Veh. Technol.*, vol. 64, no. 10, pp. 4870–4875, Oct. 2015.
[36] P. S. Koundinya, K. V. S. Hari, and L. Hanzo, "Joint design of the spatial and of the classic symbol alphabet improves single-RF spatial modulation," *IEEE Access*, vol. 4, pp. 10246–10257, 2016.
[37] B. Hassibi and B. Hochwald, "Linear dispersion codes," in *Proc. IEEE Int. Symp. Inf. Theory*, 2001, p. 325.
[38] S. Sugiura, S. Chen, and L. Hanzo, "Generalized space-time shift keying designed for flexible diversity-, multiplexing-and complexity-tradeoffs," *IEEE Trans. Wireless Commun.*, vol. 10, no. 4, pp. 1144–1153, Apr. 2011.
[39] M. Driusso, F. Babich, M. I. Kadir, and L. Hanzo, "OFDM aided space-time shift keying for dispersive downlink channels," in *Proc. IEEE Veh. Technol. Conf. (VTC Fall)*, Sep. 2012, pp. 1–5.
[40] S. Sugiura, C. Xu, S. X. Ng, and L. Hanzo, "Reduced-complexity iterative-detection-aided generalized space-time shift keying," *IEEE Trans. Veh. Technol.*, vol. 61, no. 8, pp. 3656–3664, Oct. 2012.
[41] M. I. Kadir, S. Sugiura, J. Zhang, S. Chen, and L. Hanzo, "OFDMA/SC-FDMA aided space–time shift keying for dispersive multiuser scenarios," *IEEE Trans. Veh. Technol.*, vol. 62, no. 1, pp. 408–414, Jan. 2013.
[42] R. W. Heath and A. J. Paulraj, "Linear dispersion codes for MIMO systems based on frame theory," *IEEE Trans. Signal Process.*, vol. 50, no. 10, pp. 2429–2441, Oct. 2002.
[43] P. Botsinis, S. X. Ng, and L. Hanzo, "Quantum search algorithms, quantum wireless, and a low-complexity maximum likelihood iterative quantum multi-user detector design," *IEEE Access*, vol. 1, pp. 94–122, 2013.
[44] P. Botsinis, S. X. Ng, and L. Hanzo, "Fixed-complexity quantum-assisted multi-user detection for CDMA and SDMA," *IEEE Trans. Commun.*, vol. 62, no. 3, pp. 990–1000, Mar. 2014.
[45] P. Botsinis, D. Alanis, S. X. Ng, and L. Hanzo, "Low-complexity soft-output quantum-assisted multiuser detection for direct-sequence spreading and slow subcarrier-hopping aided SDMA-OFDM systems," *IEEE Access*, vol. 2, pp. 451–472, May 2014.
[46] M. El-Hajjar and L. Hanzo, "EXIT charts for system design and analysis," *IEEE Commun. Surveys Tuts.*, vol. 16, no. 1, pp. 127–153, 1st Quart., 2014.
[47] J. Wang, X. Wang, and M. Madihian, "On the optimum design of space-time linear-dispersion codes," *IEEE Trans. Wireless Commun.*, vol. 4, no. 6, pp. 2928–2938, Nov. 2005.
[48] M. I. Kadir, S. Sugiura, S. Chen, and L. Hanzo, "Unified MIMO-multicarrier designs: A space-time shift keying approach," *IEEE Commun. Surveys Tuts.*, vol. 17, no. 2, pp. 550–579, 2nd Quart., 2015.
[49] M. K. Samimi and T. S. Rappaport, "Ultra-wideband statistical channel model for non line of sight millimeter-wave urban channels," in *Proc. IEEE Global Commun. Conf. (GLOBECOM)*, Dec. 2014, pp. 3483–3489.
[50] M. K. Samimi and T. S. Rappaport, "3-D statistical channel model for millimeter-wave outdoor mobile broadband communications," in *Proc. IEEE Int. Conf. Commun. (ICC)*, Jun. 2015, pp. 2430–2436. [Online]. Available: http://arxiv.org/abs/1503.05619
[51] M. K. Samimi and T. S. Rappaport, "Local multipath model parameters for generating 5G millimeter-wave 3GPP-like channel impulse response," in *Proc. 10th Eur. Conf. Antennas Propag. (EuCAP)*, Apr. 2016, pp. 1–5.
[52] C. Gustafson, K. Haneda, S. Wyne, and F. Tufvesson, "On mm-wave multipath clustering and channel modeling," *IEEE Trans. Antennas Propag.*, vol. 62, no. 3, pp. 1445–1455, Mar. 2014.
[53] P. Almers *et al.*, "Survey of channel and radio propagation models for wireless MIMO systems," *EURASIP J. Wireless Commun. Netw.*, vol. 2007, p. 56, Feb. 2007.
[54] M. R. Akdeniz *et al.*, "Millimeter wave channel modeling and cellular capacity evaluation," *IEEE J. Sel. Areas Commun.*, vol. 32, no. 6, pp. 1164–1179, Jun. 2014.
[55] S. Hur *et al.*, "Proposal on millimeter-wave channel modeling for 5G cellular system," *IEEE J. Sel. Topics Signal Process.*, vol. 10, no. 3, pp. 454–469, Apr. 2016.
[56] S. Sugiura and L. Hanzo, "On the joint optimization of dispersion matrices and constellations for near-capacity irregular precoded space-time shift keying," *IEEE Trans. Wireless Commun.*, vol. 12, no. 1, pp. 380–387, Jan. 2013.
[57] S. ten Brink, "Convergence behavior of iteratively decoded parallel concatenated codes," *IEEE Trans. Commun.*, vol. 49, no. 10, pp. 1727–1737, Oct. 2001.

**PANAGIOTIS BOTSINIS** (S'12–M'15) received the M.Eng. degree from the School of Electrical and Computer Engineering, National Technical University of Athens, Greece, in 2010, and the M.Sc. degree (Hons.) and the Ph.D. degree in wireless communications from the University of Southampton, U.K., in 2011 and 2015, respectively. He is currently a Research Fellow with the Southampton Wireless Group, School of Electronics and Computer Science, University of Southampton. Since 2010, he has been a member of the Technical Chamber of Greece.

His research interests include quantum-assisted communications, quantum computation, iterative detection, OFDM, MIMO, multiple access systems, coded modulation, channel coding, cooperative communications, and combinatorial optimization.

**IBRAHIM HEMADEH** received the B.Eng. degree (Hons.) in computer and communications engineering from the Islamic University of Lebanon in 2010, and the M.Sc. degree (Hons.) and the Ph.D. degree in wireless communications from the University of Southampton, U.K., in 2012 and 2017, respectively. He is currently a Research Assistant with the Southampton Wireless Research Group, Department of Electronics and Computer Science, University of Southampton. His research interests mainly include millimeter-wave communications, multi-functional MIMO, and multi-user MIMO.

**DIMITRIOS ALANIS** (S'13) received the M.Eng. degree in electrical and computer engineering from the Aristotle University of Thessaloniki in 2011, and the M.Sc. degree in wireless communications from the University of Southampton in 2012, where he is currently pursuing the Ph.D. degree with the Southampton Wireless Group, School of Electronics and Computer Science.

His research interests include quantum computation and quantum information theory, quantum search algorithms, cooperative communications, resource allocation for self-organizing networks, bioinspired optimization algorithms, and classical and quantum game theory.

**ZUNAIRA BABAR** received the B.Eng. degree in electrical engineering from the National University of Science & Technology, Islamabad, Pakistan, in 2008, and the M.Sc. degree (Hons.) and the Ph.D. degree in wireless communications from the University of Southampton, U.K., in 2011 and 2015, respectively. She is currently a Research Fellow with the Southampton Wireless Group, University of Southampton.

Her research interests include quantum error correction codes, channel coding, coded modulation, iterative detection, and cooperative communications.

**HUNG VIET NGUYEN** received the B.Eng. degree in electronics & telecommunications from the Hanoi University of Science and Technology, Hanoi, Vietnam, in 1999, the M.Eng. degree in telecommunications from the Asian Institute of Technology, Bangkok, Thailand, in 2002, and the Ph.D. degree in wireless communications from the University of Southampton, Southampton, U.K., in 2013. Since 1999, he has been a Lecturer with the Post & Telecommunications Institute of Technology, Vietnam. He is currently a Post-Doctoral Researcher with the Southampton Wireless Group, University of Southampton. He is involved in the OPTIMIX and CONCERTO European projects.

His research interests include cooperative communications, channel coding, network coding, and quantum communications.

**DARYUS CHANDRA** (S'13) received the M.Eng. degree in electrical engineering from Universitas Gadjah Mada (UGM), Indonesia, in 2014. He is currently pursuing the Ph.D. degree with the Southampton Wireless Group, School of Electronics and Computer Science, University of Southampton. He is a recipient of the Scholarship Award from Indonesia Endowment Fund for Education.

His research interests include channel codes, quantum error correction codes, and quantum communications.

**SOON XIN NG** (S'99–M'03–SM'08) received the B.Eng. degree (Hons.) in electronics engineering and the Ph.D. degree in wireless communications from the University of Southampton, Southampton, U.K., in 1999 and 2002, respectively. From 2003 to 2006, he was a Post-Doctoral Research Fellow involving in collaborative European research projects known as SCOUT, NEWCOM, and PHOENIX. Since 2006, he has been a member of Academic Staff with the School of Electronics and Computer Science, University of Southampton. He is currently an Associate Professor of telecommunications with the University of Southampton. He is involved in the OPTIMIX and CONCERTO European projects and the IUATC and UC4G projects. He has authored over 180 papers and co-authored two John Wiley/IEEE Press books in his research field.

His research interests include adaptive coded modulation, coded modulation, channel coding, space-time coding, joint source and channel coding, iterative detection, OFDM, MIMO, cooperative communications, distributed coding, quantum error correction codes, and joint wireless-and-optical-fiber communications. He is a Chartered Engineer and a fellow of the Higher Education Academy, U.K.

**MOHAMMED EL-HAJJAR** received the Ph.D. degree in wireless communications from the University of Southampton, U.K., in 2008. Following the Ph.D. degree, he joined Imagination Technologies as a Design Engineer, where he involved in designing and developing Imagination's multi-standard communications platform, which resulted in three patents. He is currently an Associate Professor with the Department of Electronics and Computer Science, University of Southampton. He has authored a Wiley–IEEE book and in excess of 80 journal and conference papers. He is a recipient of several academic awards. Mohammed's research interests include the development of intelligent communications systems, energy-efficient transceiver design, MIMO, millimeter-wave communications and Radio over fiber network design.

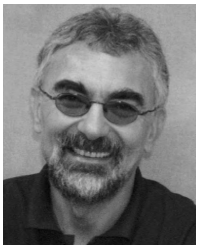

**LAJOS HANZO** (M'91–SM'92–F'04) received the degree in electronics in 1976 and the Ph.D. degree in 1983. During his 38-year career in telecommunications, he has held various research and academic posts in Hungary, Germany, and the U.K. Since 1986, he has been with the School of Electronics and Computer Science, University of Southampton, U.K., where he holds the Chair in telecommunications. He has successfully supervised about 100 Ph.D. students, co-authored 20 John Wiley/IEEE Press books on mobile radio communications totaling in excess of 10 000 pages, authored or co-authored over 1,500 research entries at the IEEE Xplore. He is currently directing a 100-strong academic research team, involving in a range of research projects in the field of wireless multimedia communications sponsored by industry, the Engineering and Physical Sciences Research Council, U.K., the European Research Council's Advanced Fellow Grant, and the Royal Society's Wolfson Research Merit Award. In 2009, he received the honorary doctorate Doctor Honoris Causa from the Technical University of Budapest. He is an enthusiastic supporter of industrial and academic liaison and he offers a range of industrial courses. He has acted both as the TPC and the General Chair of IEEE conferences, presented keynote lectures, and received a number of distinctions.

Dr. Hanzo is a fellow of the Royal Academy of Engineering, the Institution of Engineering and Technology, and the European Association for Signal Processing. He is also the Governor of the IEEE VTS. During 2008–2012, he was the Editor-in-Chief of the IEEE Press and also a Chaired Professor with Tsinghua University, Beijing. He has over 22,000 citations.